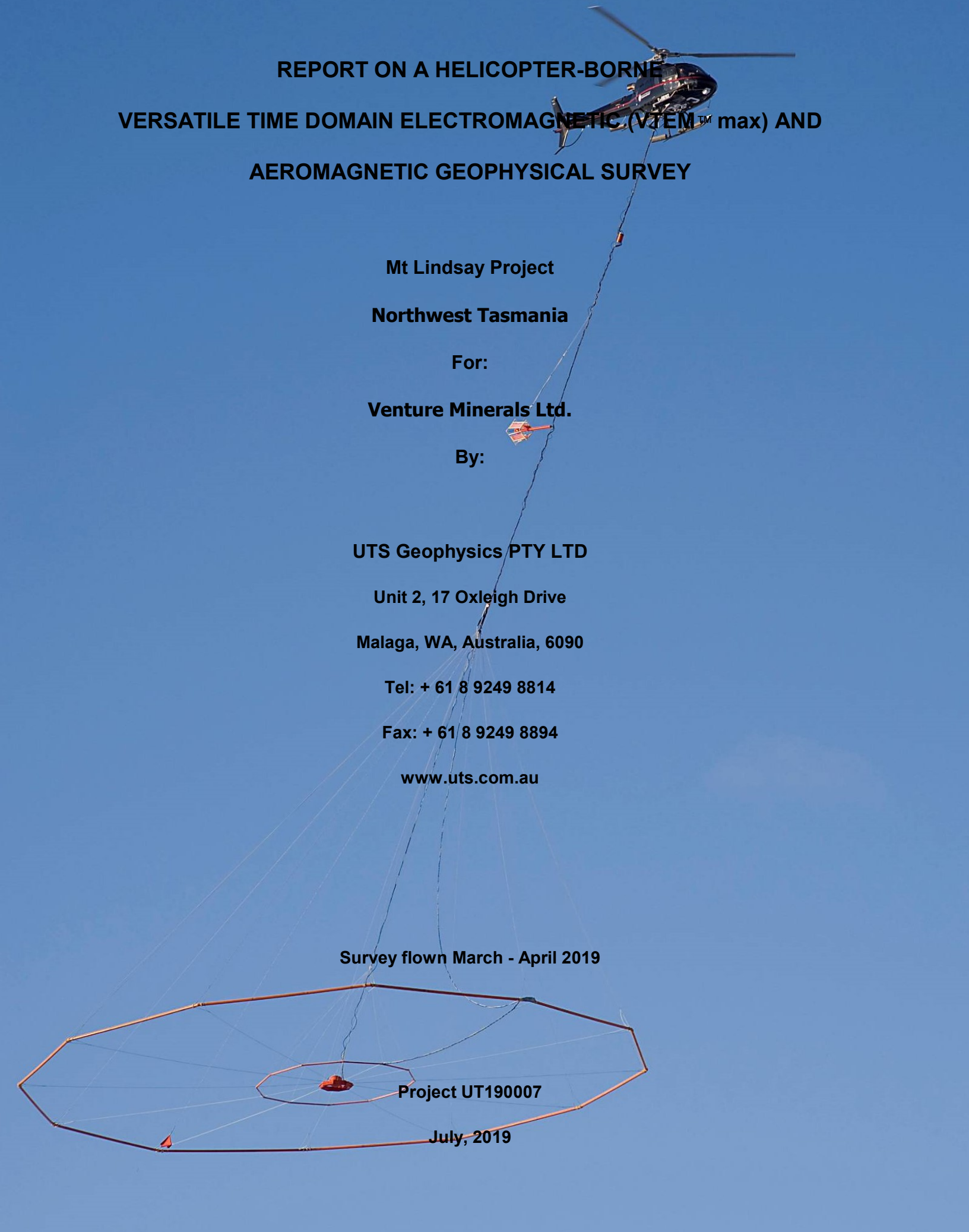

REPORT ON A HELICOPTER-BORNE VERSATILE TIME DOMAIN ELECTROMAGNETIC (VTEM™ max) AND AEROMAGNETIC GEOPHYSICAL SURVEY

Mt Lindsay Project

Northwest Tasmania

For:

Venture Minerals Ltd.

By:

UTS Geophysics PTY LTD

Unit 2, 17 Oxleigh Drive

Malaga, WA, Australia, 6090

Tel: + 61 8 9249 8814

Fax: + 61 8 9249 8894

www.uts.com.au

Survey flown March - April 2019

Project UT190007

July, 2019

TABLE OF CONTENTS

LIST OF FIGURES

LIST OF TABLES

APPENDICES

EXECUTIVE SUMMARY

MT LINDSAY PROJECT
NORTHWEST TASMANIA

During March 12th to April 23rd, 2019 UTS Geophysics Pty Ltd carried out a helicopter-borne geophysical survey over the Mt Lindsay Project area, Northwest Tasmania.

Principal geophysical sensors included a versatile time domain electromagnetic (VTEM™max) system, and a cesium magnetometer. Ancillary equipment included a GPS navigation system and a radar altimeter. A total of 677 line-kilometres (644 planned line kilometers) of geophysical data were acquired during the survey.

In-field data quality assurance and preliminary processing were carried out on a daily basis during the acquisition phase. Preliminary and final data processing, including generation of final digital data and map products were undertaken from the office of UTS Geophysics in Aurora, Ontario.

The processed survey results are presented as the following maps:

- Electromagnetic stacked profiles of the B-field Z Component,
- Electromagnetic stacked profiles of dB/dt Z Components,
- B-Field Z Component Channel grid
- Fraser Filtered dB/dt X Component Channel grid,
- Total Magnetic Intensity, Reduced to Pole (RTP)
- Calculated Time Constant (Tau) with Calculated Vertical Derivative contours,
- Resistivity Depth Images (RDI) sections are presented.

Digital data includes all electromagnetic and magnetic products, plus ancillary data including the waveform.

The survey report describes the procedures for data acquisition, description of equipment, processing, final image presentation and the specifications for the digital data set.

1. INTRODUCTION

1.1 General Considerations

UTS Geophysics Pty Ltd performed a helicopter-borne geophysical survey over Mt Lindsay Project area, Northwest Tasmania (Figure 1).

Stuart Owen represented Venture Minerals Ltd. during the data acquisition and data processing phases of this project.

The geophysical surveys consisted of helicopter borne EM using the versatile time-domain electromagnetic (VTEM™) max system with Full-Waveform processing. Measurements consisted of Vertical (Z) and In-line Horizontal (X) components of the EM fields using an induction coil and the aeromagnetic total field using a cesium magnetometer. A total of 677 line-km (644 planned line kilometers) of geophysical data were acquired during the survey.

The crew was based out of Tullah (Figure 2) in Tasmania for the acquisition phase of the survey. Survey flying started on March 12th and was completed on April 33rd, 2019.

Data quality control and quality assurance, and preliminary data processing were carried out on a daily basis during the acquisition phase of the project. Final data processing followed immediately after the end of the survey. Final reporting, data presentation and archiving were completed from the Aurora office of UTS Geophysics Pty Ltd. in July, 2019.

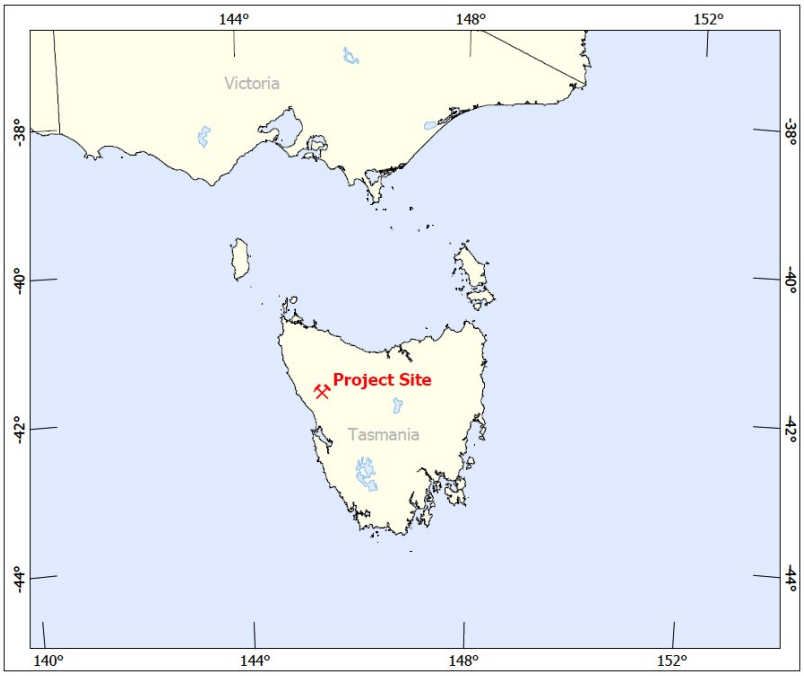

Figure 1: Property Location.

1.2 Survey and System Specifications

The survey area was located 17km west of Tullah, Tasmania (Figure 2).

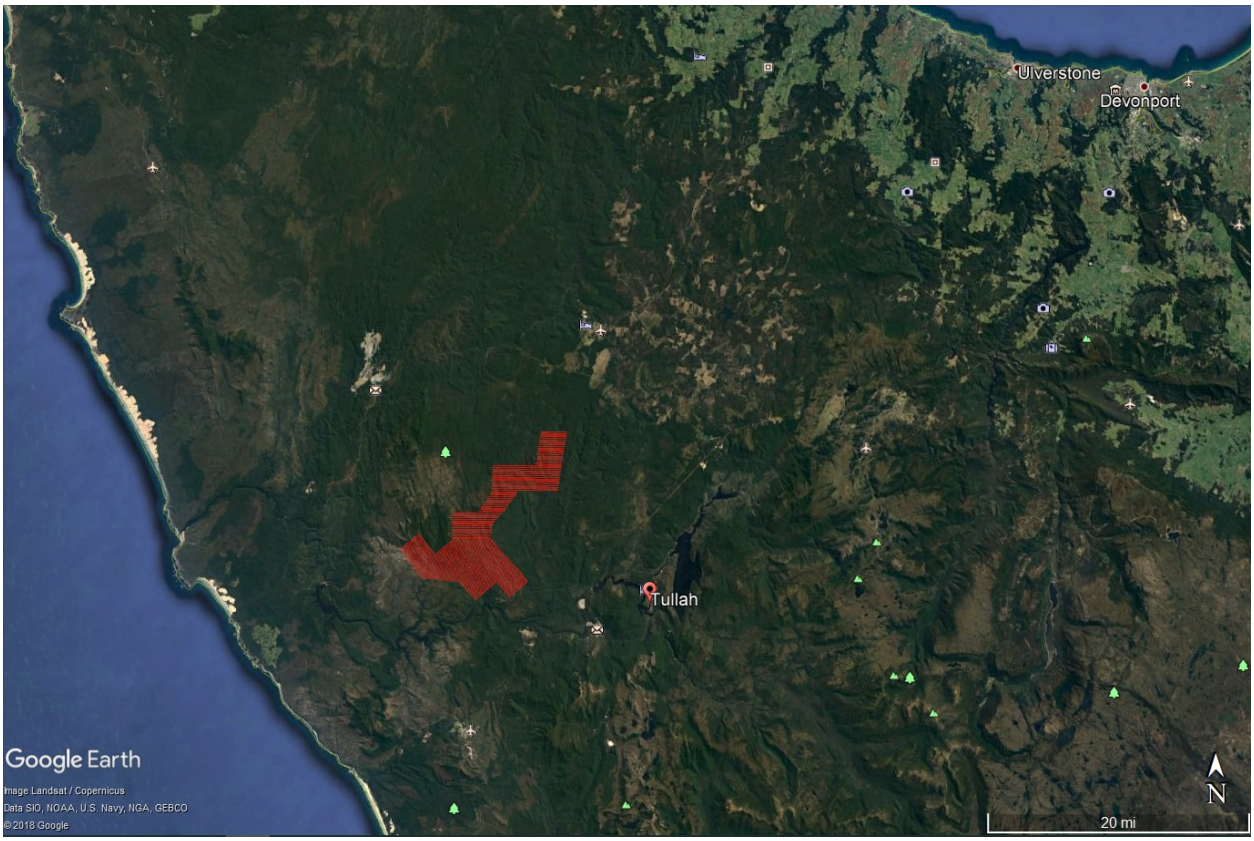

Figure 2: Survey area location on Google Earth.

The survey area was flown in a north to south (N 90° E azimuth) direction and in a northeast to southwest (N 50° E azimuth) direction, with traverse line spacing of 200 m as depicted in Figure 3. Tie lines were not planned or flown for this survey. For more detailed information on the flight spacing and direction see Table 1.

1.3 Topographic Relief and Cultural Features

Topographically, the survey area exhibit a relief with an elevation ranging from 100 to 922 metres above mean sea level over an area of 135 square kilometres (Figure 3).

There are visible signs of culture in the southeast portion of the survey area, including roads.

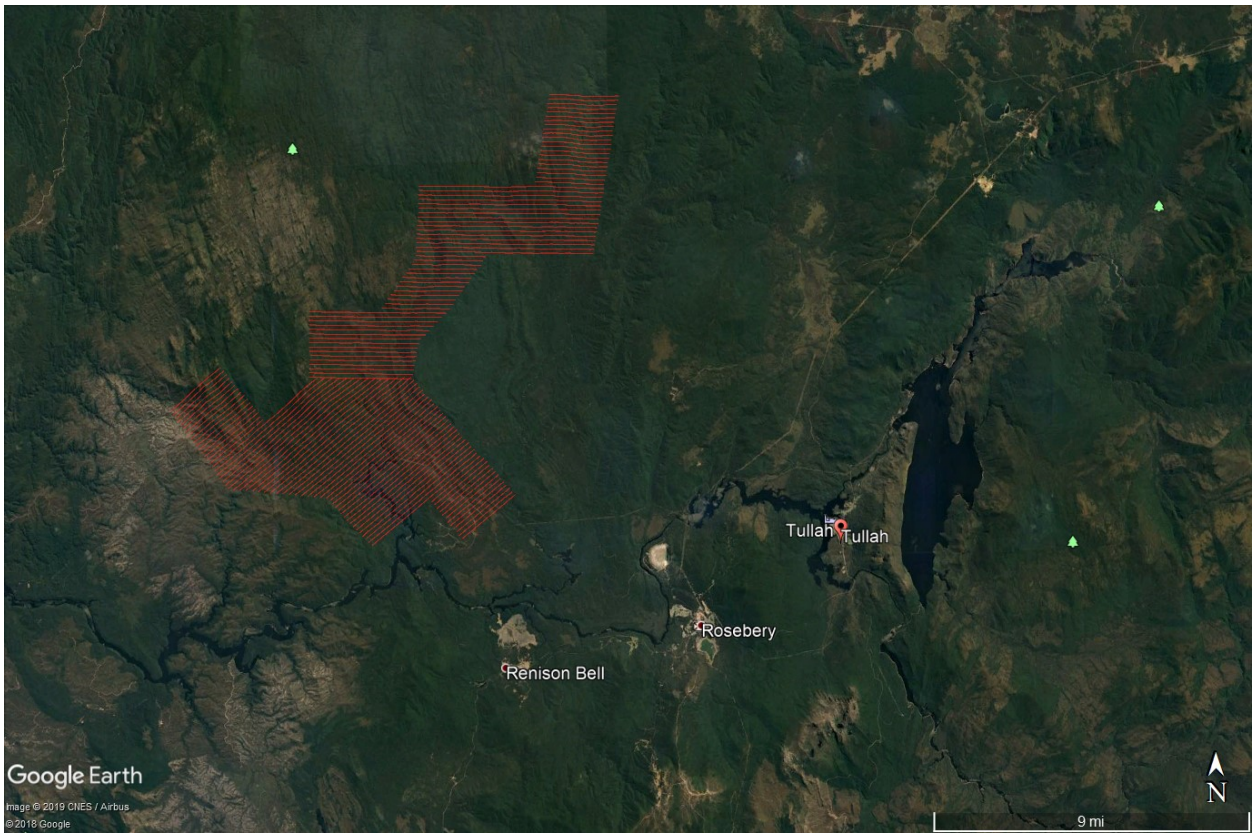

Figure 3: Flight path over a Google Earth Image

2. DATA ACQUISITION

2.1 Survey Area

The survey block (see Figure 3 and Appendix A) and general flight specifications are as follows:

Table 1: Survey Specifications

Survey block	Line spacing (m)	Area (Km^2)	Planned[1] Line-km	Actual Line-km	Flight direction	Line numbers
Mt Lindsay Project	Traverse: 200	135	664	677	N 90° E / N 270° E	L1000 - 1650
					N 50° E / N 230° E	L2000 – 2650
TOTAL		135	664	677		

Survey block boundaries co-ordinates are provided in Appendix B.

2.2 Survey Operations

Survey operations were based out of Tullah, Northwest Tasmania from March 12th to April 23rd, 2019. The following table shows the timing of the flying.

Table 2: Survey schedule

Date	Comments
3/12/2019	Mobilization
3/13/2019	Mobilization
3/14/2019	Mobilization
3/15/2019	Mobilization
3/16/2019	Mobilization
3/17/2019	Mobilization
3/18/2019	System assembly
3/19/2019	System assembly
3/20/2019	System assembly. No production due the weather.
3/21/2019	No production due to weather
3/22/2019	No production due to weather
3/23/2019	System testing.
3/24/2019	System testing.
3/25/2019	No production due the weather.
3/26/2019	No production due the weather.
3/27/2019	Test flight completed.
3/28/2019	System troubleshooting.
3/29/2019	No production due to weather.
3/30/2019	No production due to weather.

[1] Note: Actual Line kilometres represent the total line kilometres in the final database. These line-km normally exceed the planned line-km, as indicated in the survey NAV files.

Date	Comments
3/31/2019	No production due to weather.
4/1/2019	No production due to weather.
4/2/2019	Production flight aborted due to weather.
4/3/2019	No production due to weather.
4/4/2019	Production flights. Completed 3 production flights.
4/5/2019	No production due to weather.
4/6/2019	No production due to weather.
4/7/2019	No production due to weather.
4/8/2019	No production due to weather.
4/9/2019	No production due to weather.
4/10/2019	No production due to weather.
4/11/2019	No production due to weather.
4/12/2019	Production flights. Completed 2 production flights.
4/13/2019	Production flights. Completed 1 production flight.
4/14/2019	Production flights. Completed 3 production flights.
4/15/2019	No production due to weather.
4/16/2019	No production due to weather.
4/17/2019	No production due to weather.
4/18/2019	System inspection.
4/19/2019	Production flights. completed 3 production flights. Project is complete.
4/20/2019	System disassembly and demobilization.
4/21/2019	System disassembly and demobilization.
4/22/2019	Demobilization.
4/23/2019	Demobilization.

2.3 Flight Specifications

During the survey the helicopter was maintained at a mean altitude of 159 metres above the ground with an average survey speed of 86 km/hour. This allowed for an actual average transmitter-receiver loop terrain clearance of 111 metres and a magnetic sensor clearance of 121 metres.

The on board operator was responsible for monitoring the system integrity. He also maintained a detailed flight log during the survey, tracking the times of the flight as well as any unusual geophysical or topographic features.

On return of the aircrew to the base camp the survey data was transferred from a compact flash card (PCMCIA) to the data processing computer. The data were then uploaded via ftp to the UTS office in Aurora for daily quality assurance and quality control by qualified personnel.

2.4 Aircraft and Equipment

2.4.1 Survey Aircraft

The survey was flown using a Eurocopter AS 350 B3 helicopter, registration VH-VOX. The helicopter is owned and operated by United Aero Helicopters. Installation of the geophysical and ancillary equipment was carried out by a UTS Geophysics Pty Ltd crew.

2.4.2 Electromagnetic System

The electromagnetic system was a UTS Time Domain EM (VTEM^{TM}max) full receiver-waveform streamed data recorded system. The "full waveform VTEM^{TM} system" uses the streamed half-cycle recording of transmitter and receiver waveforms to obtain a complete system response calibration throughout the entire survey flight. VTEM^{TM}, with the serial number 12 had been used for the survey. The configuration is as indicated in Figure 5.

The VTEM^{TM} max Receiver and transmitter coils were in concentric-coplanar and Z-direction oriented configuration. The receiver system for the project also included coincident-coaxial X-direction coils to measure the in-line dB/dt and calculate B-Field responses. The EM transmitter-receiver loop was towed at a mean distance of 111 metres below the aircraft as shown in Figure 5: **VTEMTMmax System Configuration.**.The receiver decay recording scheme is shown in Figure 4.

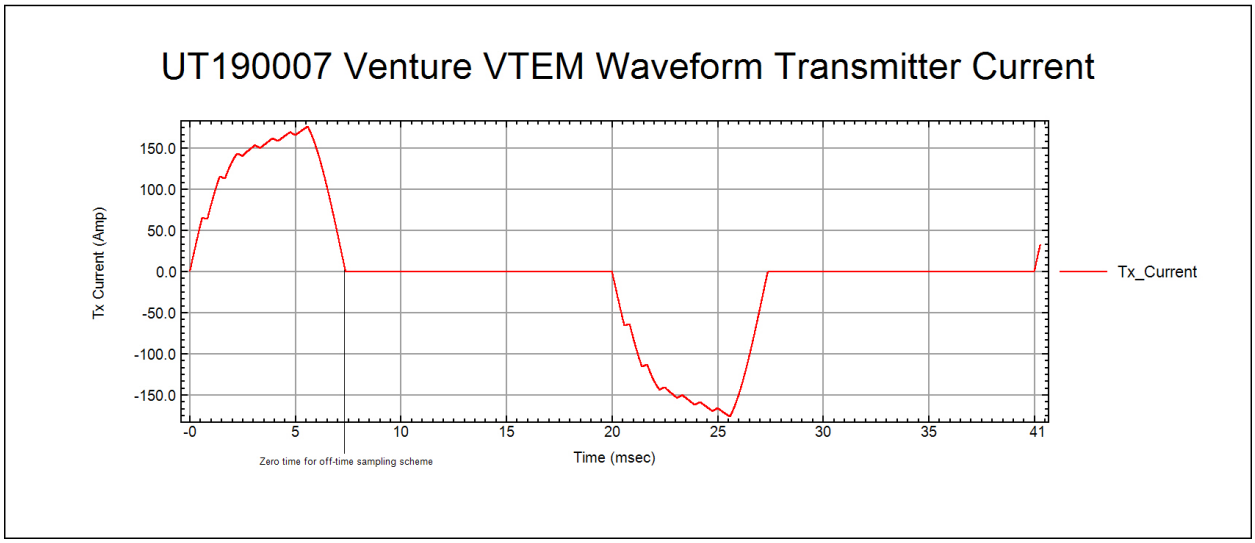

Figure 4: VTEM^{TM} Waveform & Sample Times

The VTEM^{TM} decay sampling scheme is shown in

Table 3 below. Forty five time measurement gates were used for the final data processing in the range from 0.021 to 10.667 msec. Zero time for off-time sampling scheme is equal to current pulse width and defined as the time near the end of the turn-off ramp where the dI/dt waveform falls to 1/2 of its peak value".

Table 3: Off-Time Decay Sampling Scheme

VTEM™ Decay Sampling Scheme				
index	**Start**	**End**	**Middle**	**Window**
Miliseconds				
4	0.018	0.023	0.021	0.005
5	0.023	0.029	0.026	0.005
6	0.029	0.034	0.031	0.005
7	0.034	0.039	0.036	0.005
8	0.039	0.045	0.042	0.006
9	0.045	0.051	0.048	0.007
10	0.051	0.059	0.055	0.008
11	0.059	0.068	0.063	0.009
12	0.068	0.078	0.073	0.010
13	0.078	0.090	0.083	0.012
14	0.090	0.103	0.096	0.013
15	0.103	0.118	0.110	0.015
16	0.118	0.136	0.126	0.018
17	0.136	0.156	0.145	0.020
18	0.156	0.179	0.167	0.023
19	0.179	0.206	0.192	0.027
20	0.206	0.236	0.220	0.030
21	0.236	0.271	0.253	0.035
22	0.271	0.312	0.290	0.040
23	0.312	0.358	0.333	0.046
24	0.358	0.411	0.383	0.053
25	0.411	0.472	0.440	0.061
26	0.472	0.543	0.505	0.070
27	0.543	0.623	0.580	0.081
28	0.623	0.716	0.667	0.093
29	0.716	0.823	0.766	0.107
30	0.823	0.945	0.880	0.122
31	0.945	1.086	1.010	0.141
32	1.086	1.247	1.161	0.161
33	1.247	1.432	1.333	0.185
34	1.432	1.646	1.531	0.214
35	1.646	1.891	1.760	0.245
36	1.891	2.172	2.021	0.281
37	2.172	2.495	2.323	0.323
38	2.495	2.865	2.667	0.370
39	2.865	3.292	3.063	0.427
40	3.292	3.781	3.521	0.490
41	3.781	4.341	4.042	0.560

VTEM™ Decay Sampling Scheme				
index	Start	End	Middle	Window
Miliseconds				
42	4.341	4.987	4.641	0.646
43	4.987	5.729	5.333	0.742
44	5.729	6.581	6.125	0.852
45	6.581	7.560	7.036	0.979
46	7.560	8.685	8.083	1.125

Z Component: 4-46 time gates
X Component: 20-46 time gates

VTEM^{TM} max system specification:

Transmitter

- Transmitter loop diameter: 35 m
- Effective Transmitter loop area: 3761 m^2
- Number of turns: 4
- Transmitter base frequency: 25 Hz
- Peak current: 176.3 A
- Pulse width: 7.36 ms
- Wave form shape: trapezoid
- Peak dipole moment: 678,508 nIA
- Average transmitter-receiver loop terrain clearance: 111 metres

Receiver

X Coil diameter: 0.32 m

- Number of turns: 245
- Effective coil area: 19.69 m^2

Z-Coil diameter: 1.2 m

- Number of turns: 100
- Effective coil area: 113.04 m^2

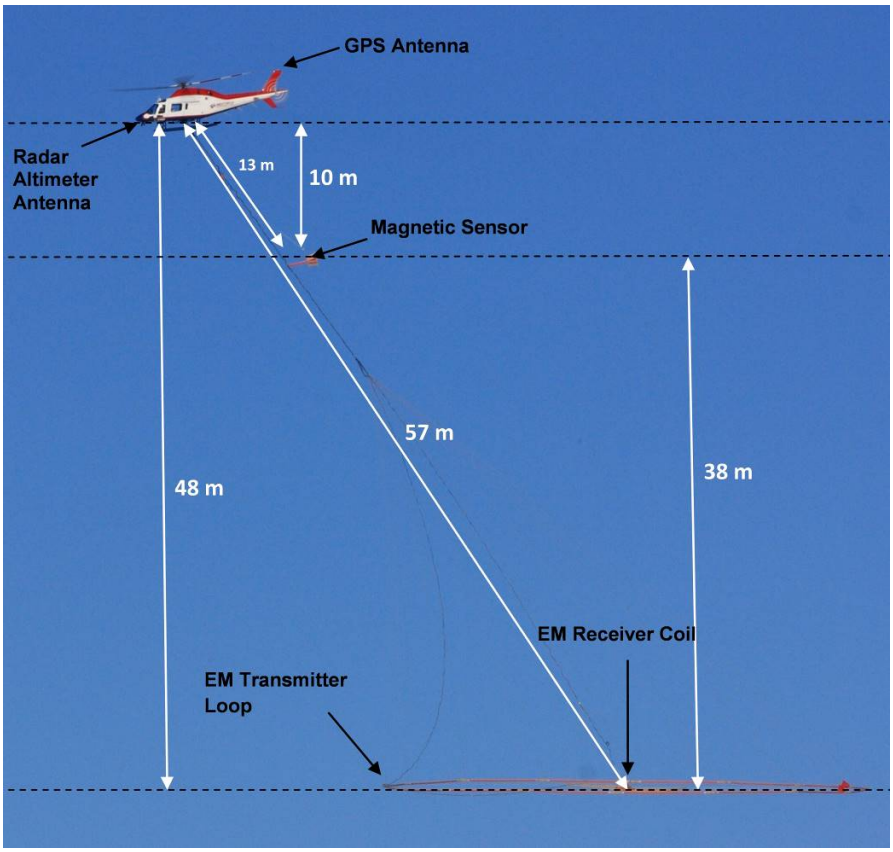

Figure 5: VTEM^{TM} max System Configuration.

2.4.3 Airborne magnetometer

The magnetic sensor utilized for the survey was Geometrics optically pumped cesium vapour magnetic field sensor mounted 10 metres below the helicopter, as shown in Figure 5. The sensitivity of the magnetic sensor is 0.02 nanoTesla (nT) at a sampling interval of 0.1 seconds.

2.4.4 Full Waveform VTEM™ Sensor Calibration

The calibration is performed on the complete VTEM™ system installed in and connected to the helicopter, using special calibration equipment. This calibration takes place on the ground at the start of the project prior to surveying.

The procedure takes half-cycle files acquired and calculates a calibration file consisting of a single stacked half-cycle waveform. The purpose of the stacking is to attenuate natural and man-made magnetic signals, leaving only the response to the calibration signal.

This calibration allows the transfer function between the EM receiver and data acquisition system and also the transfer function of the current monitor and data acquisition system to be determined. These calibration results are then used in VTEM™ full waveform processing.

2.4.5 Radar Altimeter

A Terra TRA 3000/TRI 40 radar altimeter was used to record terrain clearance. The antenna was mounted beneath the bubble of the helicopter cockpit (Figure 5).

2.4.6 GPS Navigation System

The navigation system used was a UTS PC104 based navigation system utilizing a NovAtel's WAAS (Wide Area Augmentation System) enabled GPS receiver, UTS navigate software, a full screen display with controls in front of the pilot to direct the flight and a NovAtel GPS antenna mounted on the helicopter tail (Figure 5). As many as 11 GPS and two WAAS satellites may be monitored at any one time. The positional accuracy or circular error probability (CEP) is 1.8 m, with WAAS active, it is 1.0 m. The co-ordinates of the block were set-up prior to the survey and the information was fed into the airborne navigation system.

2.4.7 Digital Acquisition System

A UTS data acquisition system recorded the digital survey data on an internal compact flash card. Data is displayed on an LCD screen as traces to allow the operator to monitor the integrity of the system. The data type and sampling interval as provided in Table 4.

Table 4: Acquisition Sampling Rates

Data Type	Sampling
TDEM	0.1 sec
Magnetometer	0.1 sec
GPS Position	0.1 sec
Radar Altimeter	0.2 sec

2.5 Base Station

A combined magnetometer/GPS base station was utilized on this project. A Geometrics Cesium vapour magnetometer was used as a magnetic sensor with a sensitivity of 0.001 nT. The base station was recording the magnetic field together with the GPS time at 1 Hz on a base station computer.

The base station magnetometer sensor was located away from electric transmission lines and moving ferrous objects such as motor vehicles. The base station data were backed-up to the data processing computer at the end of each survey day.

3. PERSONNEL

The following UTS Ltd. personnel were involved in the project.

Field:

Project Manager:	Hayley Kelly (Office)
Data QC:	Neil Fiset (Office)
Crew chief:	Peter MacDonald
Operator:	Jared White

The survey pilot and the mechanical engineer were employed directly by the helicopter operator – United Aero Helicopters

Pilot:	Hugh Gifford
Mechanical Engineer:	Contracted third party provider

Office:

Preliminary Data Processing:	Neil Fiset
Final Data Processing:	Julian Boada
Data QA/QC:	Kanita Khaled, P.Geo
Reporting/Mapping:	Joseli Soares

Processing phases were carried out under the supervision of Kanita Khaled (P.Geo). The customer relations were looked after by Levin Lee.

4. DATA PROCESSING AND PRESENTATION

Data compilation and processing were carried out by the application of Geosoft OASIS Montaj and programs proprietary to UTS Ltd.

4.1 Flight Path

The flight path, recorded by the acquisition program as WGS84 latitude/longitude, was converted into GDA 94 MGA Zone 55 coordinate system in Oasis Montaj.

The flight path was drawn using linear interpolation between x, y positions from the navigation system. Positions are updated every second and expressed as UTM easting's (x) and UTM northing's (y).

4.2 Electromagnetic Data

The Full Waveform EM specific data processing operations included:

- Half cycle stacking (performed at time of acquisition);
- System response correction;
- Parasitic and drift removal by deconvolution.

A three stage digital filtering process was used to reject major sferic events and to reduce system noise. Local sferic activity can produce sharp, large amplitude events that cannot be removed by conventional filtering procedures. Smoothing or stacking will reduce their amplitude but leave a broader residual response that can be confused with geological phenomena. To avoid this possibility, a computer algorithm searches out and rejects the major sferic events.

The signal to noise ratio was further improved by the application of a low pass linear digital filter. This filter has zero phase shift which prevents any lag or peak displacement from occurring, and it suppresses only variations with a wavelength less than about 1 second or 15 metres. This filter is a symmetrical 1 sec linear filter.

The results are presented as stacked profiles of EM voltages for the time gates, in linear - logarithmic scale for the B-field Z component and dB/dt responses in the Z, X and Y components. B-field Z component time channel recorded at 0.667 milliseconds after the termination of the impulse is also presented as contour colour images. Fraser Filter X component is also presented as a colour image. Calculated Time Constant (TAU) with Calculated Vertical Derivative RTP contours is presented in Appendix C and E. Resistivity Depth Image (RDI) is also presented in Appendix F and G.

VTEM^{TM} max has three receiver coil orientations. Z-axis coil is oriented parallel to the transmitter coil axis and both are horizontal to the ground. The X-axis coil is oriented parallel to the ground and along the line-of-flight. The Y-axis coil is oriented parallel to the ground and perpendicular to the line-of-flight. The combination of the X, Y and Z coils configuration provides information on the position, depth, dip and thickness of a conductor. This combined three coil configuration provides information on the position, depth, dip and thickness of a conductor. Generalized modeling results of VTEM^{TM} max data are shown in Appendix D.

In general X-component data produce cross-over type anomalies: from "+ to – "in flight direction of flight for "thin" sub vertical targets and from "- to +" in direction of flight for "thick" targets. Z component data produce double peak type anomalies for "thin" sub vertical targets and single peak for "thick" targets.

The limits and change-over of "thin-thick" depends on dimensions of a TEM system.

Because of X component polarity is under line-of-flight, convolution Fraser filter (FF, Figure 6) is applied to X component data to represent axes of conductors in the form of grid map. In this case positive FF anomalies always correspond to "plus-to-minus" X data crossovers independently of direction of flight.

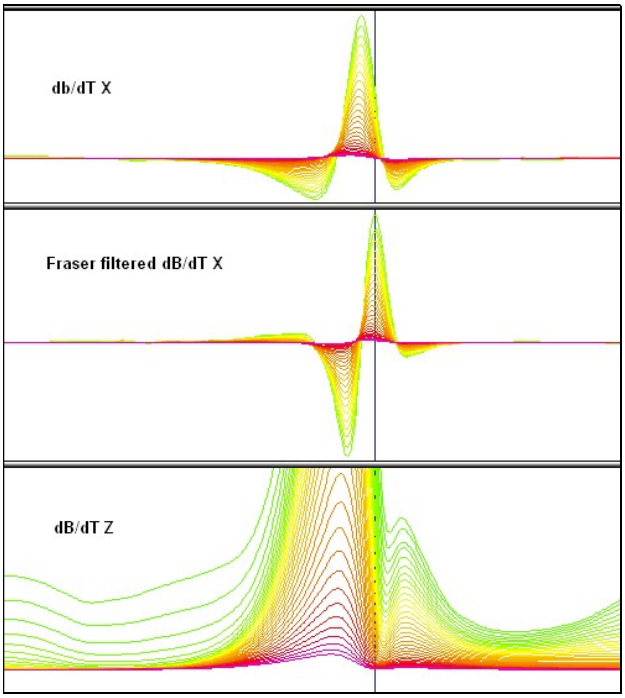

Figure 6: Z, X and Fraser filtered X (FFx) components for "thin" target.

4.3 Magnetic Data

The processing of the magnetic data involved the correction for diurnal variations by using the digitally recorded ground base station magnetic values. The base station magnetometer data was edited and merged into the Geosoft GDB database on a daily basis. The aeromagnetic data was corrected for diurnal variations by subtracting the observed magnetic base station deviations.

The corrected magnetic data was interpolated between survey lines using a random point gridding method to yield x-y grid values for a standard grid cell size of approximately 50 metres at the mapping scale. The Minimum Curvature algorithm was used to interpolate values onto a rectangular regular spaced grid.

4.4 TAU Parameter and CVG Calculation

The processed VTEM^{TM}survey results are presented as a calculated dB/dt time constant (Tau), which is an indicator of geological unit's electrical conductance.

An explanation of the EM time constant calculation is provided in Appendix F. The TAU dB/dt map is presented as Figure D-6 in Appendix D and in Appendix C. The map is accompanied by an overlay of the calculated vertical gradient (Reduced to Pole) of TMI anomaly contours for tracing possible EM-MAG anomaly correlations.

The CVG_RTP contour layer, on the top of TAU color grid, generally is more representative of the smaller scale and shallower magnetic sources in comparison with the TMI. CVG is designed to emphasize the structures and lithological units that might not otherwise be seen on the TMI due to the nearby presence of stronger magnetic responses, showing a high resolution in terms of individual structures.

5. DELIVERABLES

5.1 Survey Report

The survey report describes the data acquisition, processing, and final presentation of the survey results. The survey report is provided in two paper copies and digitally in PDF format.

5.2 Maps

Final maps were produced at a scale of 1:20,000 for best representation of the survey size and line spacing. The coordinate/projection system used was GDA 94 Datum, MGA Zone 55. All maps show the flight path trace and topographic data; latitude and longitude are also noted on maps.

The preliminary and final results of the survey are presented as EM profiles, a late-time gate gridded EM channel, and a colour magnetic TMI contour map.

- Maps at 1:20,000 in Geosoft MAP format, as follows:

UT190007_20k_dBdt:	dB/dt profiles Z Component, Time Gates 0.220 – 7.036 ms in linear – logarithmic scale.
UT190007_20k_BField:	B-field profiles Z Component, Time Gates 0.220 – 7.036 ms in linear – logarithmic scale over Total Magnetic Intensity
UT190007_20k_CVG_RTP:	Calculated Vertical Gradient (CVG) of Reduced to Pole (RTP) Total Magnetic Intensity
UT190007_20k_BFz35:	B-field late time Z Component Channel 35, Time Gate 1.760 ms
UT190007_20k_RTP:	Total Magnetic Intensity Reduced to Pole
UT190007_20k_SFxFF25:	Fraser Filtered dB/dt X Component, Channel 25, Time Gate 0.440 ms

UT190007_20k_SFz25: dB/dt Z Component Channel 25 (Time Gate 0.440 ms)

UT190007_20k_TauSF_RTP_CVG: dB/dt Calculated Time Constant (Tau) with Calculated Vertical Derivative of RTP contours

- Maps are also presented in PDF format.

- Topographic data base was derived from Geoscience Australia 1:250,000 scale (www.ga.gov.au)
- A Google Earth file *UT190007_Venture.kml* showing the flight path of the block is included. Free versions of Google Earth software from: http://earth.google.com/download-earth.html

5.3 Digital Data

- Two copies of the data and maps on DVD were prepared to accompany the report. Each DVD contains a digital file of the line data in GDB Geosoft Montaj format as well as the maps in Geosoft Montaj Map and PDF format.

  DVD structure:
  Data contains databases, grids and maps, as described below.
  Report contains a copy of the report and appendices in PDF format.

  Databases in Geosoft GDB format, containing the channels listed in Table 5.

Table 5: Geosoft GDB Data Format

Channel name	Units	Description
X	metres	GDA 94 Easting - MGA Zone 55
Y	metres	GDA 94 Northing - MGA Zone 55
Longitude:	Decimal Degrees	WGS 84 Longitude data
Latitude:	Decimal Degrees	WGS 84 Latitude data
Z:	metres	GPS antenna elevation (above Geoid)
Zb:	metres	EM bird elevation (above Geoid)
Radar:	metres	helicopter terrain clearance from radar altimeter
Radarb:	metres	Calculated EM transmitter-receiver loop terrain clearance from radar altimeter
DEM:	metres	Digital Elevation Model
Gtime:	Seconds of the day	GPS time
Mag1:	nT	Raw Total Magnetic field data
Basemag:	nT	Magnetic diurnal variation data
Mag2:	nT	Diurnal corrected Total Magnetic field data
Mag3:	nT	Levelled Total Magnetic field data
CVG	nT/m	Calculated Vertical Derivative of TMI.
RTP:	nT	Reduced to Pole (RTP) of TMI
CVG_RTP:	nT/m	Calculated Vertical Derivative of RTP TMI
SFz[4]:	pV/(A*m^4)	Z dB/dt 0.021 millisecond time channel
SFz[5]:	pV/(A*m^4)	Z dB/dt 0.026 millisecond time channel
SFz[6]:	pV/(A*m^4)	Z dB/dt 0.031 millisecond time channel
SFz[7]:	pV/(A*m^4)	Z dB/dt 0.036 millisecond time channel

Channel name	Units	Description
SFz[8]:	pV/(A*m^4)	Z dB/dt 0.042 millisecond time channel
SFz[9]:	pV/(A*m^4)	Z dB/dt 0.048 millisecond time channel
SFz[10]:	pV/(A*m^4)	Z dB/dt 0.055 millisecond time channel
SFz[11]:	pV/(A*m^4)	Z dB/dt 0.063 millisecond time channel
SFz[12]:	pV/(A*m^4)	Z dB/dt 0.073 millisecond time channel
SFz[13]:	pV/(A*m^4)	Z dB/dt 0.083 millisecond time channel
SFz[14]:	pV/(A*m^4)	Z dB/dt 0.096 millisecond time channel
SFz[15]:	pV/(A*m^4)	Z dB/dt 0.110 millisecond time channel
SFz[16]:	pV/(A*m^4)	Z dB/dt 0.126 millisecond time channel
SFz[17]:	pV/(A*m^4)	Z dB/dt 0.145 millisecond time channel
SFz[18]:	pV/(A*m^4)	Z dB/dt 0.167 millisecond time channel
SFz[19]:	pV/(A*m^4)	Z dB/dt 0.192 millisecond time channel
SFz[20]:	pV/(A*m^4)	Z dB/dt 0.220 millisecond time channel
SFz[21]:	pV/(A*m^4)	Z dB/dt 0.253 millisecond time channel
SFz[22]:	pV/(A*m^4)	Z dB/dt 0.290 millisecond time channel
SFz[23]:	pV/(A*m^4)	Z dB/dt 0.333 millisecond time channel
SFz[24]:	pV/(A*m^4)	Z dB/dt 0.383 millisecond time channel
SFz[25]:	pV/(A*m^4)	Z dB/dt 0.440 millisecond time channel
SFz[26]:	pV/(A*m^4)	Z dB/dt 0.505 millisecond time channel
SFz[27]:	pV/(A*m^4)	Z dB/dt 0.580 millisecond time channel
SFz[28]:	pV/(A*m^4)	Z dB/dt 0.667 millisecond time channel
SFz[29]:	pV/(A*m^4)	Z dB/dt 0.766 millisecond time channel
SFz[30]:	pV/(A*m^4)	Z dB/dt 0.880 millisecond time channel
SFz[31]:	pV/(A*m^4)	Z dB/dt 1.010 millisecond time channel
SFz[32]:	pV/(A*m^4)	Z dB/dt 1.161 millisecond time channel
SFz[33]:	pV/(A*m^4)	Z dB/dt 1.333 millisecond time channel
SFz[34]:	pV/(A*m^4)	Z dB/dt 1.531 millisecond time channel
SFz[35]:	pV/(A*m^4)	Z dB/dt 1.760 millisecond time channel
SFz[36]:	pV/(A*m^4)	Z dB/dt 2.021 millisecond time channel
SFz[37]:	pV/(A*m^4)	Z dB/dt 2.323 millisecond time channel
SFz[38]:	pV/(A*m^4)	Z dB/dt 2.667 millisecond time channel
SFz[39]:	pV/(A*m^4)	Z dB/dt 3.063 millisecond time channel
SFz[40]:	pV/(A*m^4)	Z dB/dt 3.521 millisecond time channel
SFz[41]:	pV/(A*m^4)	Z dB/dt 4.042 millisecond time channel
SFz[42]:	pV/(A*m^4)	Z dB/dt 4.641 millisecond time channel
SFz[43]:	pV/(A*m^4)	Z dB/dt 5.333 millisecond time channel
SFz[44]:	pV/(A*m^4)	Z dB/dt 6.125 millisecond time channel
SFz[45]:	pV/(A*m^4)	Z dB/dt 7.036 millisecond time channel
SFz[46]:	pV/(A*m^4)	Z dB/dt 8.083 millisecond time channel
SFx[20]:	pV/(A*m^4)	X dB/dt 0.220 millisecond time channel
SFx[21]:	pV/(A*m^4)	X dB/dt 0.253 millisecond time channel
SFx[22]:	pV/(A*m^4)	X dB/dt 0.290 millisecond time channel
SFx[23]:	pV/(A*m^4)	X dB/dt 0.333 millisecond time channel
SFx[24]:	pV/(A*m^4)	X dB/dt 0.383 millisecond time channel
SFx[25]:	pV/(A*m^4)	X dB/dt 0.440 millisecond time channel
SFx[26]:	pV/(A*m^4)	X dB/dt 0.505 millisecond time channel
SFx[27]:	pV/(A*m^4)	X dB/dt 0.580 millisecond time channel
SFx[28]:	pV/(A*m^4)	X dB/dt 0.667 millisecond time channel
SFx[29]:	pV/(A*m^4)	X dB/dt 0.766 millisecond time channel
SFx[30]:	pV/(A*m^4)	X dB/dt 0.880 millisecond time channel
SFx[31]:	pV/(A*m^4)	X dB/dt 1.010 millisecond time channel

Channel name	Units	Description
SFx[32]:	pV/(A*m^4)	X dB/dt 1.161 millisecond time channel
SFx[33]:	pV/(A*m^4)	X dB/dt 1.333 millisecond time channel
SFx[34]:	pV/(A*m^4)	X dB/dt 1.531 millisecond time channel
SFx[35]:	pV/(A*m^4)	X dB/dt 1.760 millisecond time channel
SFx[36]:	pV/(A*m^4)	X dB/dt 2.021 millisecond time channel
SFx[37]:	pV/(A*m^4)	X dB/dt 2.323 millisecond time channel
SFx[38]:	pV/(A*m^4)	X dB/dt 2.667 millisecond time channel
SFx[39]:	pV/(A*m^4)	X dB/dt 3.063 millisecond time channel
SFx[40]:	pV/(A*m^4)	X dB/dt 3.521 millisecond time channel
SFx[41]:	pV/(A*m^4)	X dB/dt 4.042 millisecond time channel
SFx[42]:	pV/(A*m^4)	X dB/dt 4.641 millisecond time channel
SFx[43]:	pV/(A*m^4)	X dB/dt 5.333 millisecond time channel
SFx[44]:	pV/(A*m^4)	X dB/dt 6.125 millisecond time channel
SFx[45]:	pV/(A*m^4)	X dB/dt 7.036 millisecond time channel
SFx[46]:	pV/(A*m^4)	X dB/dt 8.083 millisecond time channel
BFz	(pV*ms)/(A*m^4)	Z B-Field data for time channels 4 to 48
BFx	(pV*ms)/(A*m^4)	X B-Field data for time channels 20 to 48
SFxFF	pV/(A*m4)	Fraser filtered X dB/dt
NchanBF		Last channel where the algorithm stops calculation, B-Field
TauBF	milliseconds	Time Constant (Tau) calculated from B-field data
NchanSF		Last channel where the algorithm stops calculation, dB/dt
TauSF	milliseconds	Time Constant (Tau) calculated from dB/dt data
PLM:		50 Hz power line monitor

Electromagnetic B-field and dB/dt Z component data is found in array channel format between indexes 4 – 46, and X component data from 20 – 46, as described above.

- Database of the Resistivity Depth Images in Geosoft GDB format, containing the following channels:

Table 6: Geosoft Apparent Resistivity Depth Image GDB Data Format

Channel name	Units	Description
Xg	metres	GDA 94 Easting - MGA Zone 55
Yg	metres	GDA 94 Northing - MGA Zone 55
Dist:	meters	Distance from the beginning of the line
Depth:	meters	array channel, depth from the surface
Z:	meters	array channel, depth from sea level
AppRes:	Ohm-m	array channel, Apparent Resistivity
TR:	meters	EM system height from sea level
Topo:	meters	digital elevation model
Radarb:	metres	Calculated EM transmitter-receiver loop terrain clearance from radar altimeter
SF:	pV/(A*m^4)	array channel, dB/dT
Mag:	nT	TMI data
CVG:	nT/m	CVG data
PLM:		50Hz Power Line Monitor
DOI:	Metres	Depth of Investigation: a measure of VTEM depth effectiveness

- Database of the VTEM™ Waveform “UT190007_waveform.gdb” in Geosoft GDB format, containing the following channels:

  Time: Sampling rate interval, 5.2083 microseconds
  Tx_Current: Output current of the transmitter (Amp)

- Grids in Geosoft GRD, GeoTIFF format, as follows:

UT190007_BFz35:	B-Field Z Component Channel 35 (Time Gate 1.760 ms)
UT190007_CVG_RTP:	Calculated Vertical Derivative of RTP TMI (nT/m)
UT190007_DEM:	Digital Elevation Model (metres)
UT190007_PLM:	Power Line Monitor
UT190007_RTP:	Total Magnetic Intensity (nT) Reduced to the Pole
UT190007_SFxFF25:	Fraser Filter X Component dB/dt Channel 25 (Time Gate 0.440 ms)
UT190007_SFz15:	dB/dt Z Component Channel 15 (Time Gate 0.110ms)
UT190007_SFz25:	dB/dt Z Component Channel 25 (Time Gate 0.440ms)
UT190007_SFz41:	dB/dt Z Component Channel 41 (Time Gate 4.042 ms)
UT190007_TauBF:	B-Field Calculated Time Constant (ms)
UT190007_TauSF:	dB/dt Calculated Time Constant (ms)

A Geosoft .GRD file has a .GI metadata file associated with it, containing grid projection information. A grid cell size of 50 metres was used.

6. CONCLUSIONS AND RECOMMENDATIONS

A helicopter-borne versatile time domain electromagnetic (VTEM^{TM}Max) geophysical survey has been completed over Mt Lindsay Project area for Venture Minerals Ltd. situated at Tullah, Northwest Tasmania.

The total area coverage is 135 km^2. Total survey line coverage is 677 line kilometres. The principal geophysical sensors included a Full Waveform Time Domain electromagnetic system, and a magnetometer. Results have been presented as stacked profiles, and contour color images at a scale of 1:20,000.

Based on the geophysical results obtained, the dB/dt time constant tau and all dB/dt time channels shows several electromagnetic anomalous areas spread throughout the block. Early Time channels show additional anomalies in the Northwest and center of the block. Most anomalies have a strong magnetic influence. Northern anomalies have apparent resistivity values that range between 4-12 ohm-m. Southern anomalies have apparent resistivity values that range between 2-6 ohm-m. In some areas the electromagnetic anomalies correspond to magnetic anomalous zones, as seen on the Tau – CVG image UT190007_20K_TauSF.pdf.

If the anomalous zones correspond to an exploration model on the area it is recommended performing 1D EM Inversions and 3D Magnetic Vectorized Inversion (MVI) planning prior to ground follow up and drill testing.

Respectfully submitted[2],

Neil Fiset
UTS Ltd.

Julian Boada
UTS Ltd.

PROFESSIONAL GEOSCIENTIST
KANITA KHALED
PRACTISING MEMBER
2995
ONTARIO

Kanita Khaled
UTS Ltd.

Joseli Soares
UTS Ltd.

July, 2019

[2] Final data processing of the EM and magnetic data were carried out by Emily Data, under the supervision of Kanita Khaled, P.Geo, from the office of UTS Geophysics in Aurora, Ontario

APPENDIX A

SURVEY BLOCK LOCATION MAP

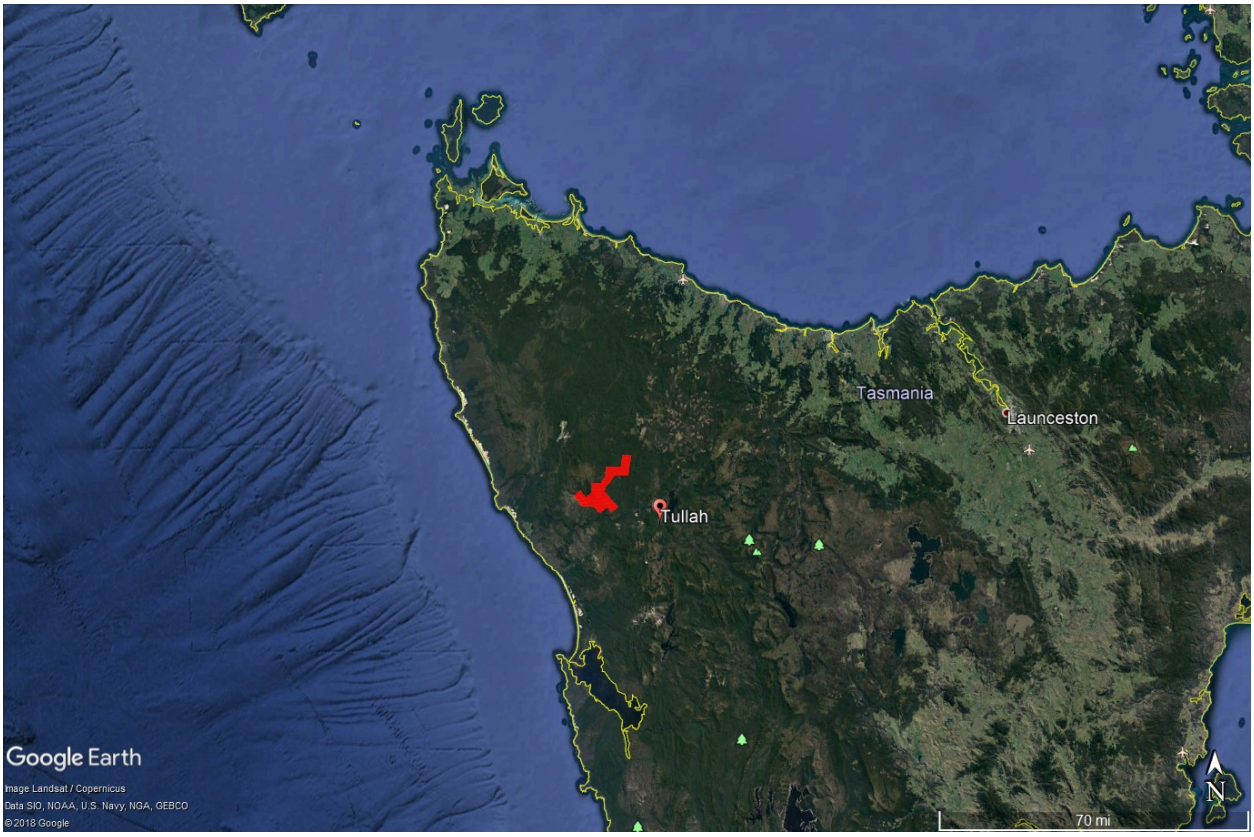

Survey Overview of the Survey Area

APPENDIX B

SURVEY BLOCK COORDINATES

(WGS 84, UTM Zone 55 South)

Ramsay	
X	Y
374670	5397984
371610	5397969
371000	5393718
365646	5393744
365556	5390235
363998	5388086
360720	5388076
360783	5384830
365230	5384830
365602	5386624
366984	5388086
368600	5390511
373527	5390593

Lindsay	
X	Y
360738	5384827
358541	5382821
356554	5385407
354281	5383434
357057	5379813
361525	5379451
363736	5377151
366369	5379380
367806	5377651
370014	5379521
365239	5384919

APPENDIX C - GEOPHYSICAL MAPS[1]

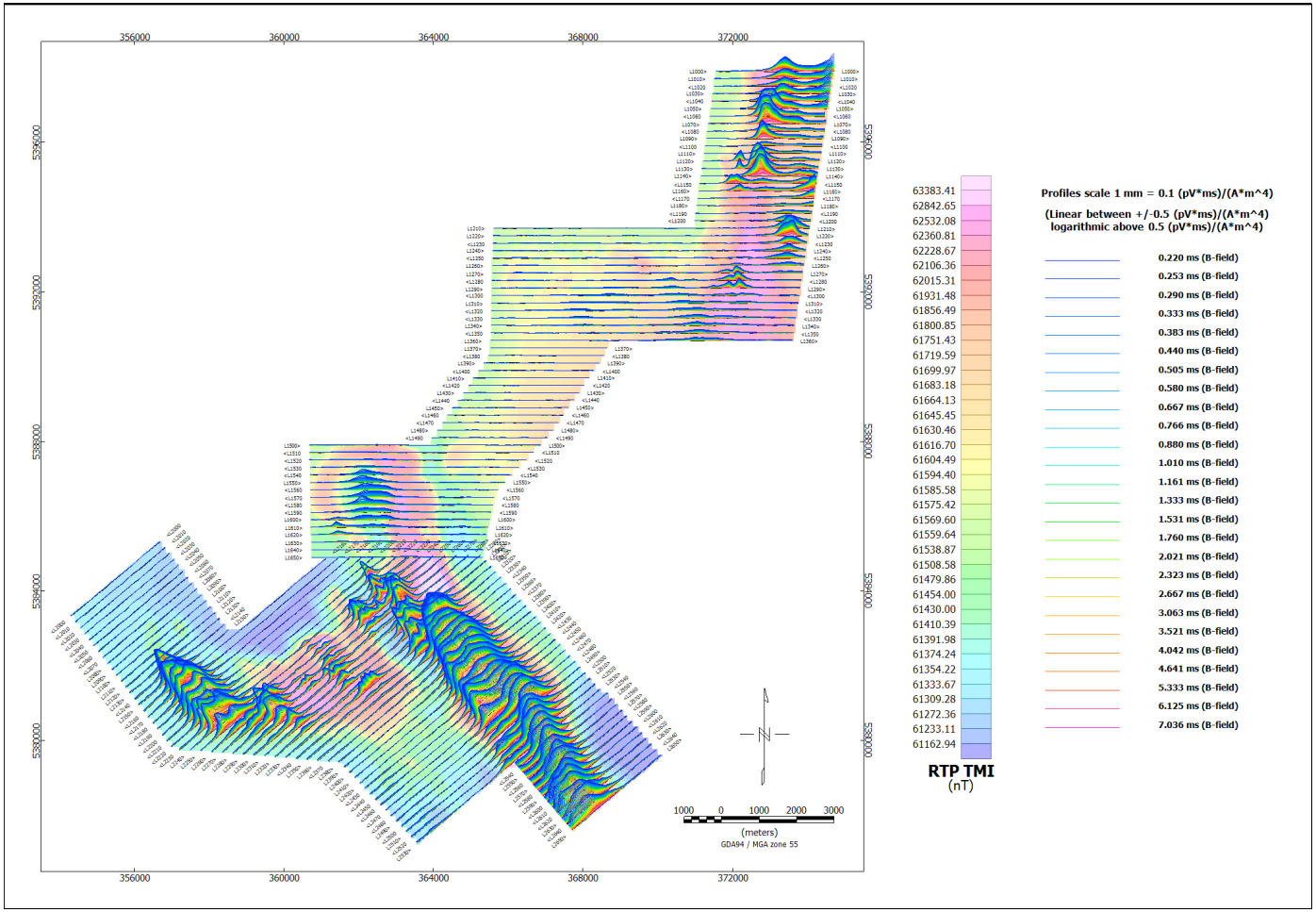

B-field profiles Z Component, Time Gates 0.220 – 7.036 ms in linear – logarithmic scale

[1] Full size geophysical maps are also available in PDF format on the final DVD

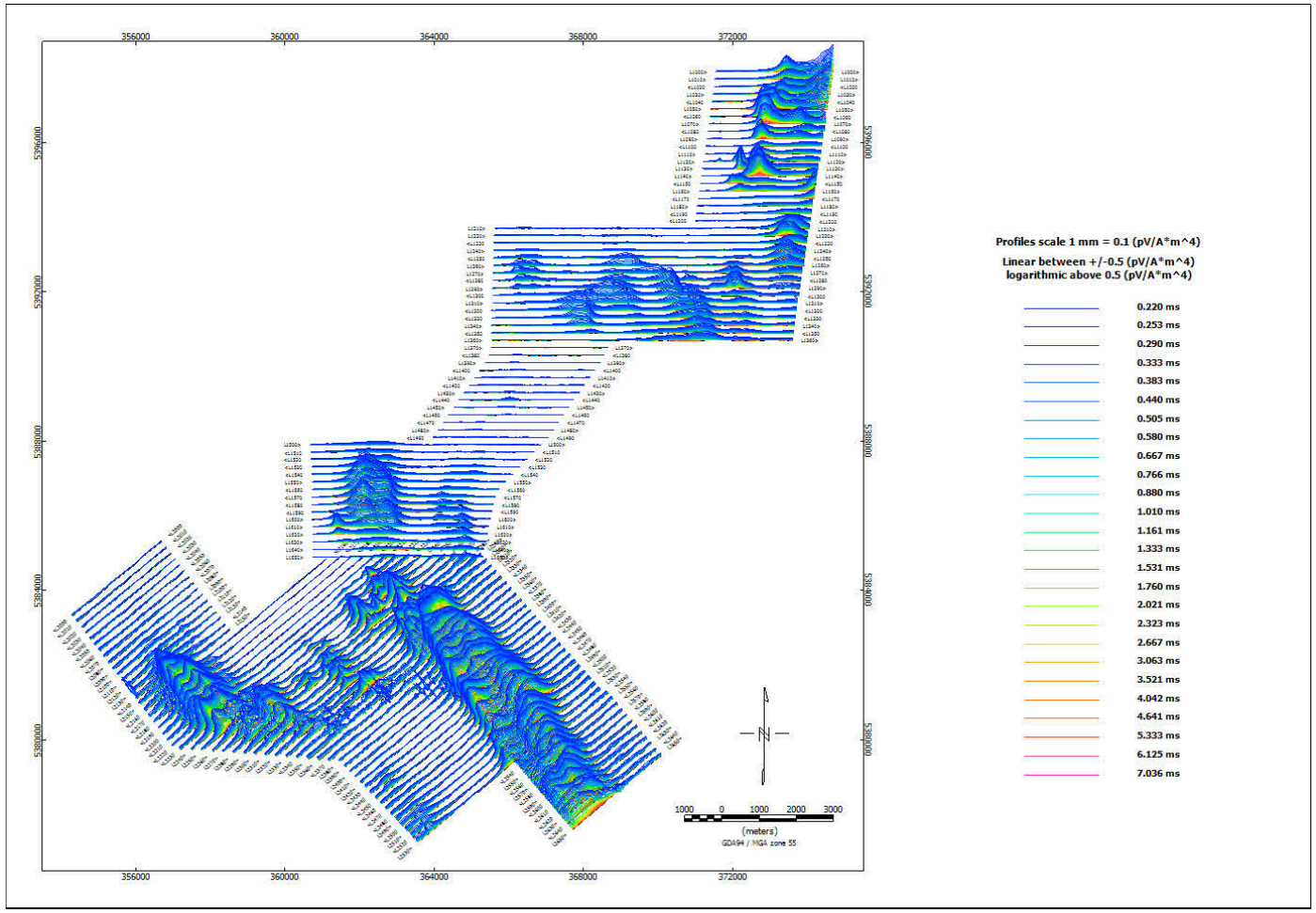

dB/dt profiles Z Component, Time Gates 0.220 – 7.036 ms in linear – logarithmic scale

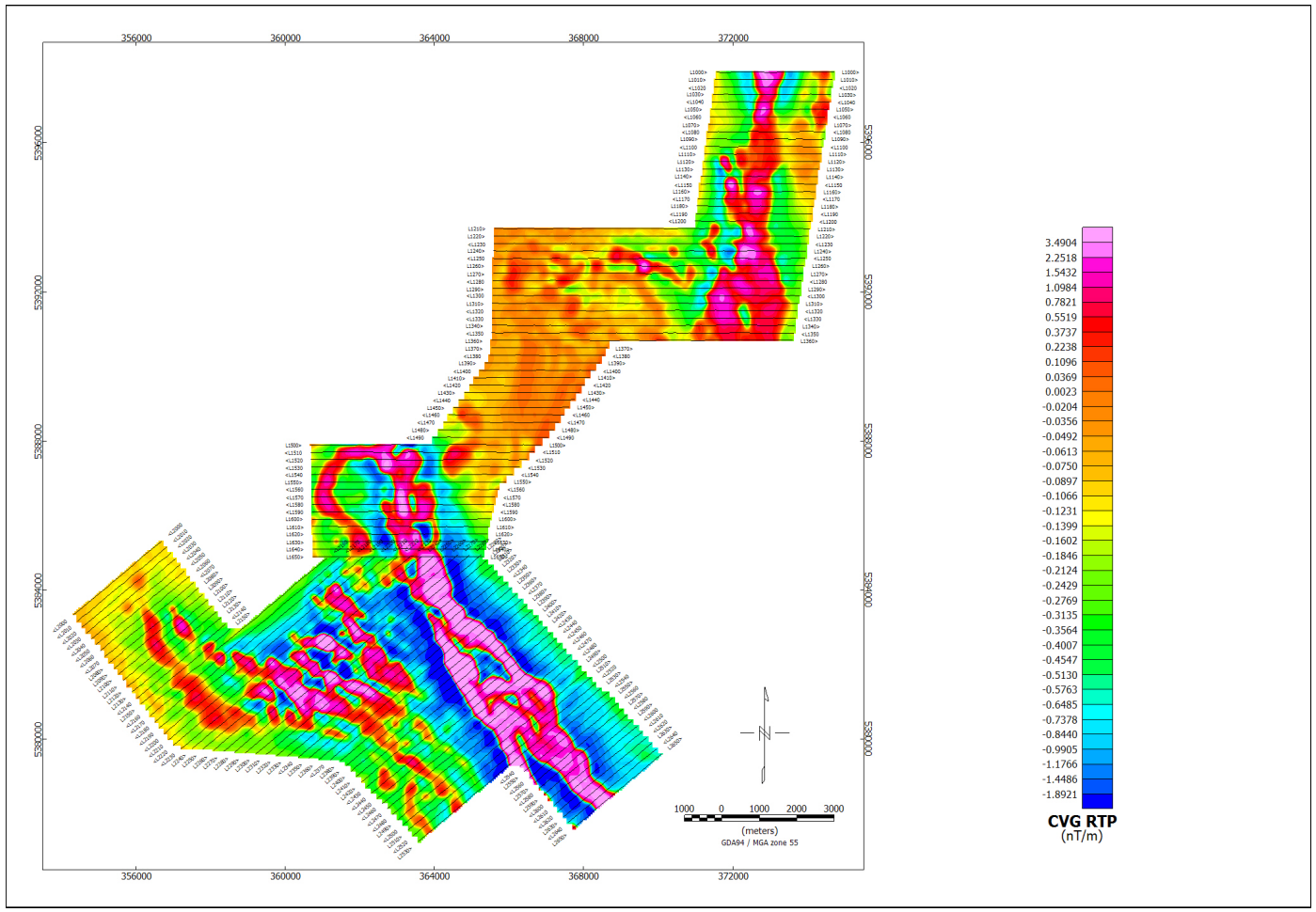

Calculated Vertical Gradient (CVG) Reduced to Pole (RTP)

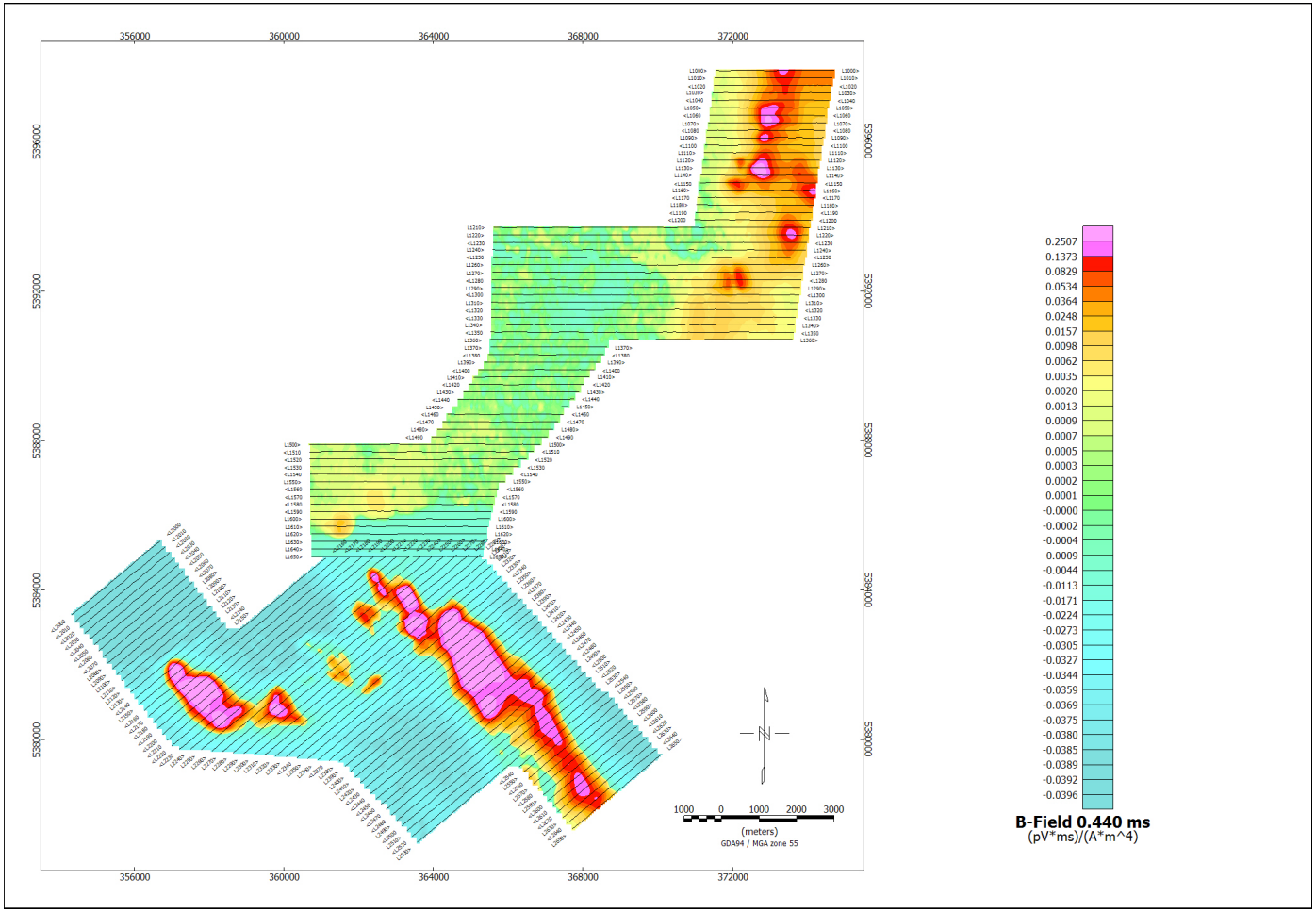

B-field late time Z Component Channel 35, Time Gate 1.760 ms

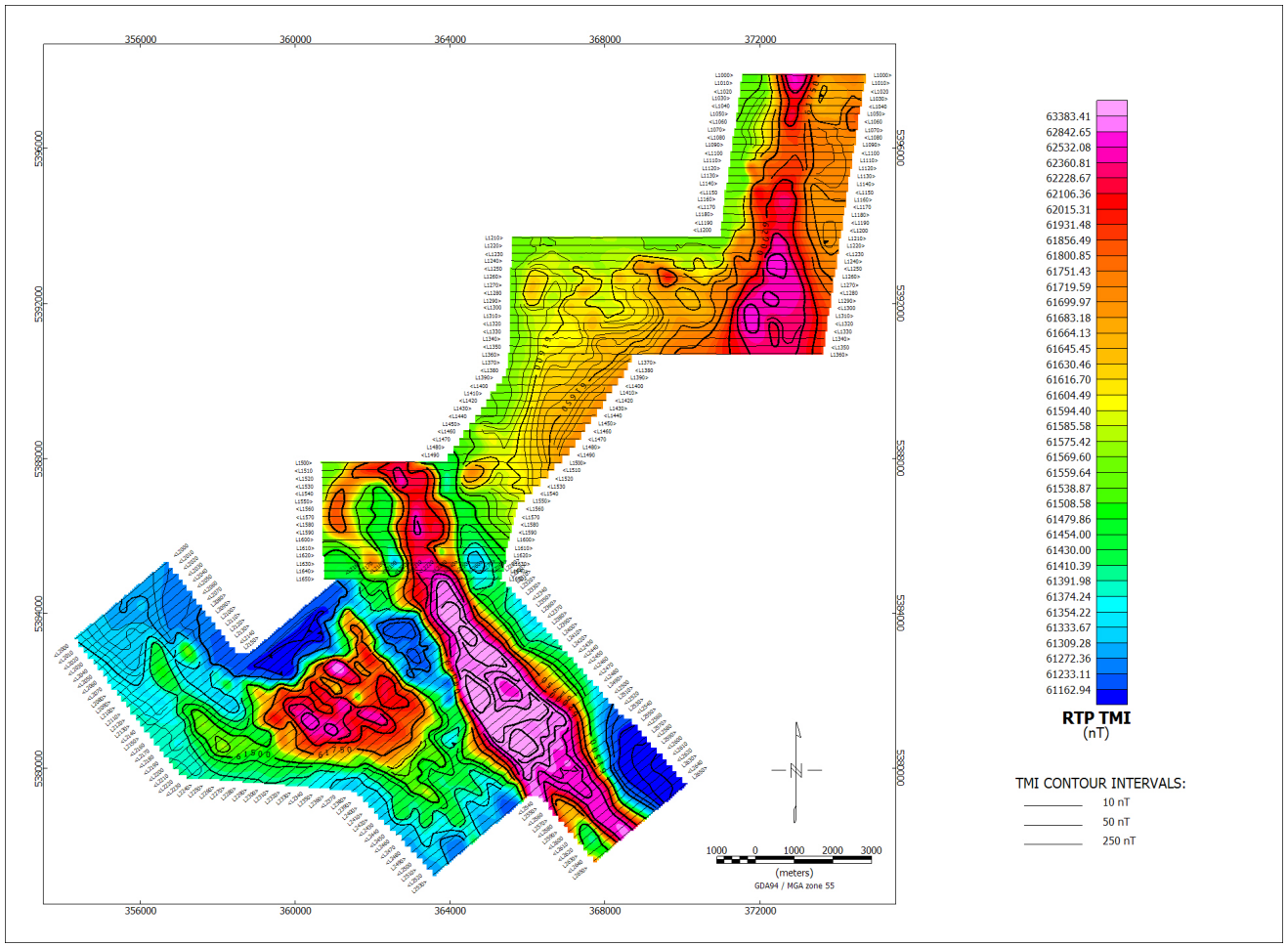

Total Magnetic Intensity (TMI) Reduced to Pole (RTP)

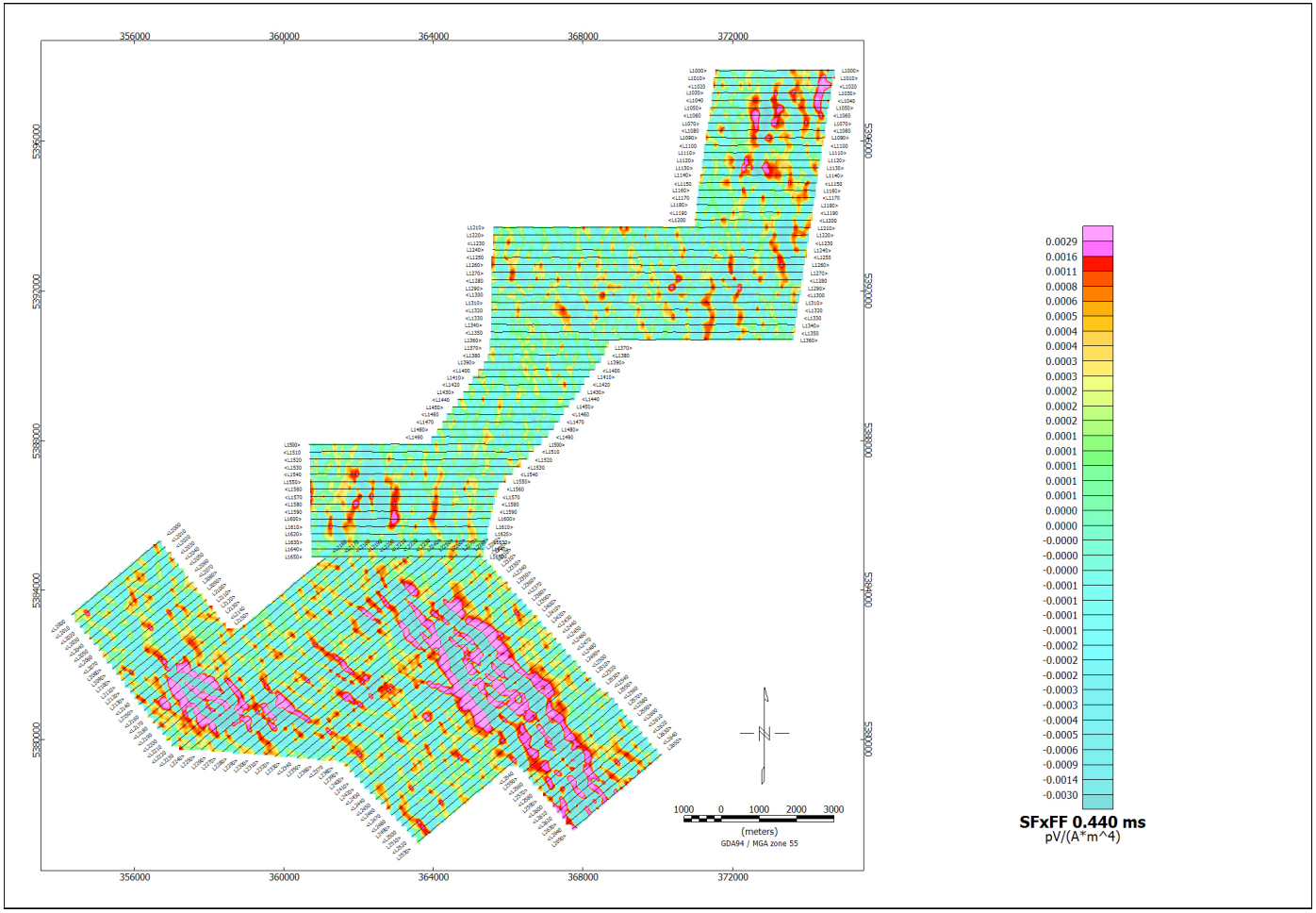

Fraser Filtered dB/dt X Component, Channel 25, Time Gate 0.440 ms

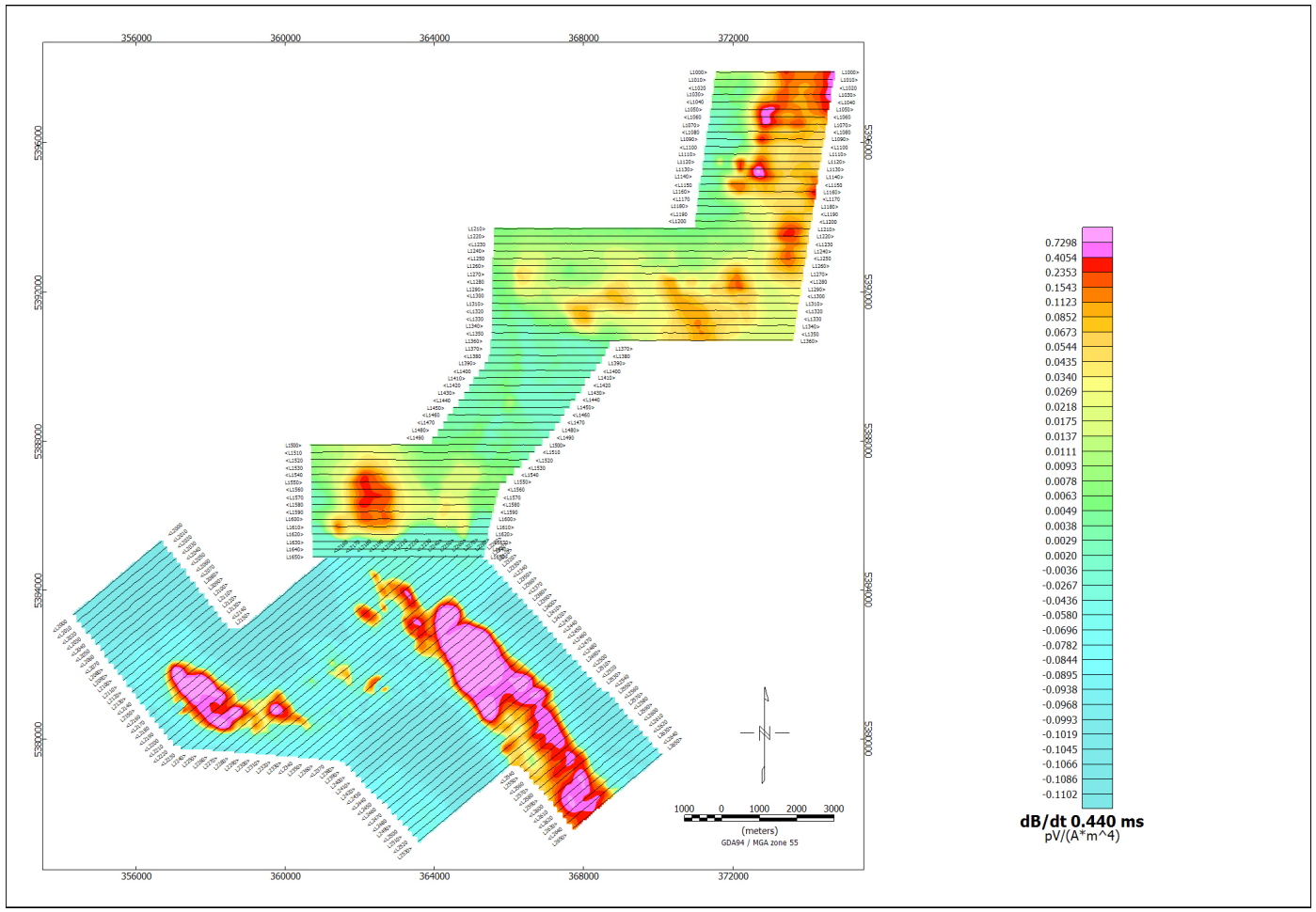

dB/dt Z Component Channel 25 (Time Gate 0.440 ms)

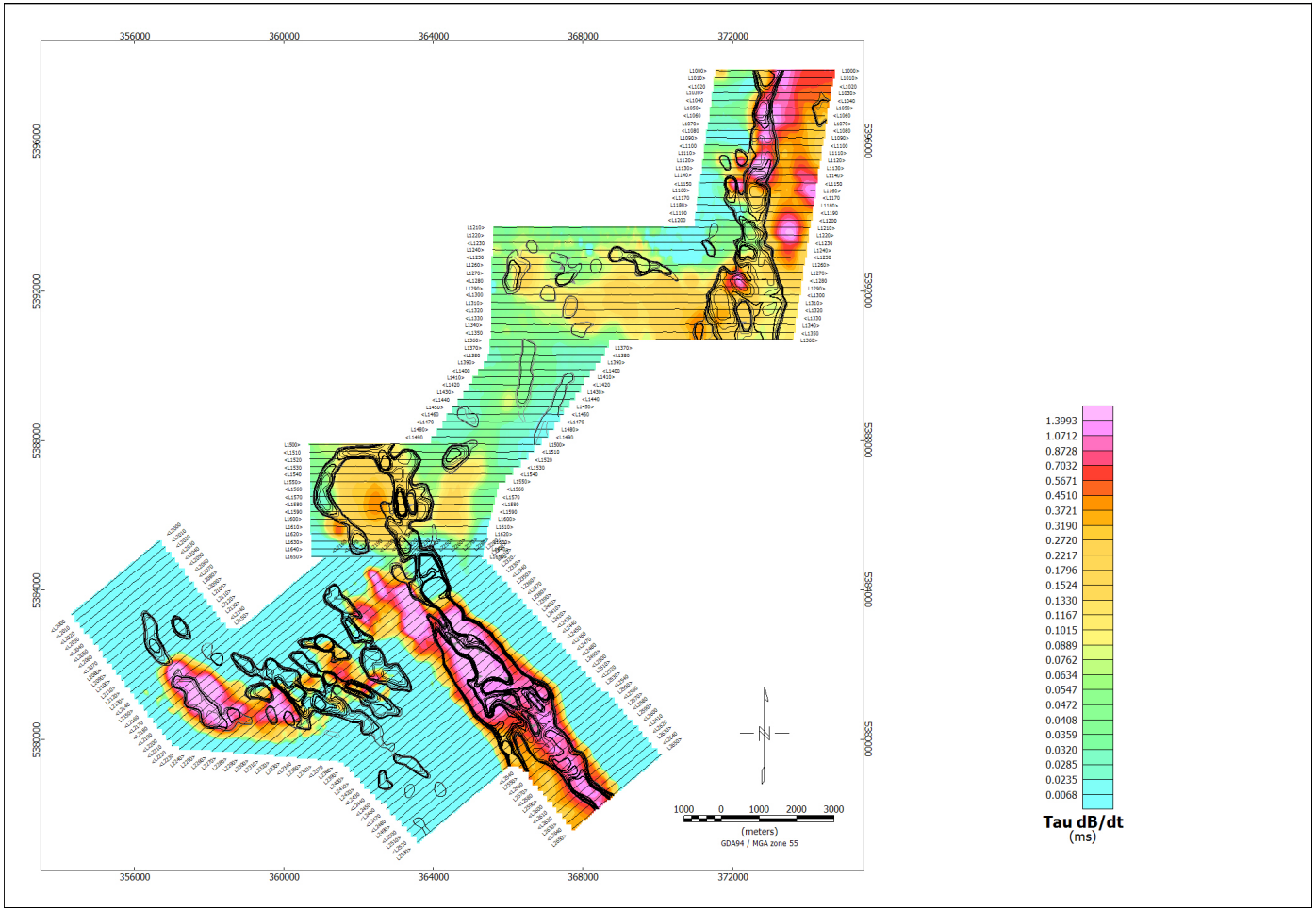

dB/dT Calculated Time Constant (Tau) with Calculated Vertical Derivative contours

APPARENT RESISTIVITY DEPTH IMAGE (RDI) MAPS

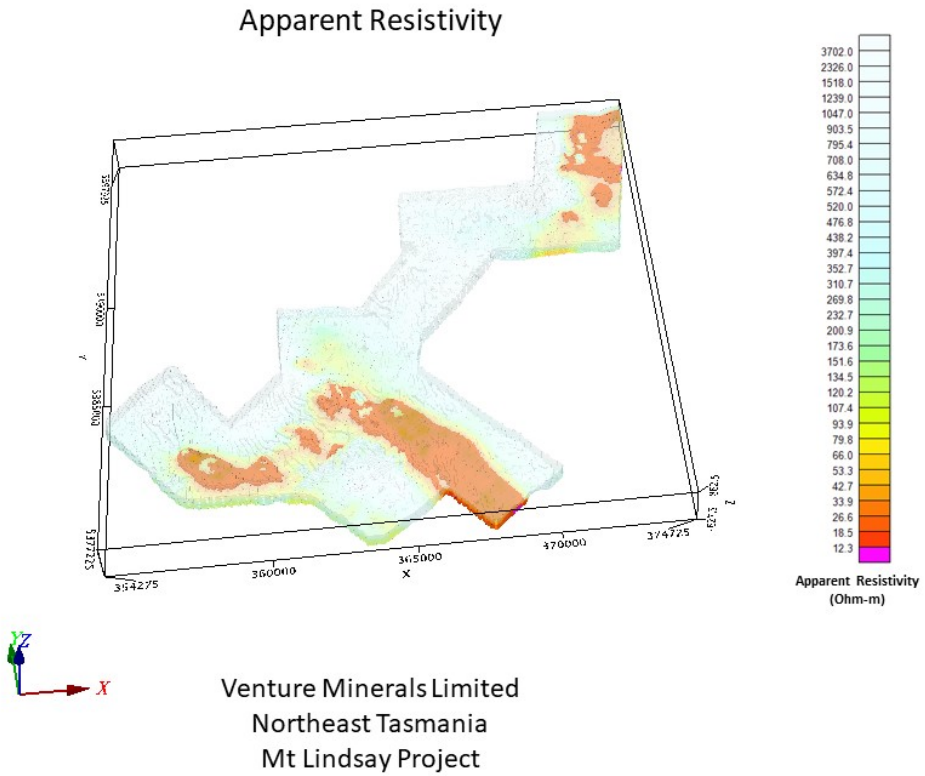

3D View of Apparent Resistivity Depth Image (RDI) Voxel

APPENDIX D

GENERALIZED MODELING RESULTS OF THE VTEM™ SYSTEM

Introduction

The VTEM™ system is based on a concentric or central loop design, whereby, the receiver is positioned at the centre of a transmitter loop that produces a primary field. The wave form is a bi-polar, modified square wave with a turn-on and turn-off at each end.

During turn-on and turn-off, a time varying field is produced (dB/dt) and an electro-motive force (emf) is created as a finite impulse response. A current ring around the transmitter loop moves outward and downward as time progresses. When conductive rocks and mineralization are encountered, a secondary field is created by mutual induction and measured by the receiver at the centre of the transmitter loop.

Efficient modeling of the results can be carried out on regularly shaped geometries, thus yielding close approximations to the parameters of the measured targets. The following is a description of a series of common models made for the purpose of promoting a general understanding of the measured results.

A set of models has been produced for the UTS VTEM™ system dB/dT Z and X components (see models D1 to D15). The Maxwell ™ modeling program (EMIT Technology Pty. Ltd. Midland, WA, AU) used to generate the following responses assumes a resistive half-space. The reader is encouraged to review these models, so as to get a general understanding of the responses as they apply to survey results. While these models do not begin to cover all possibilities, they give a general perspective on the simple and most commonly encountered anomalies.

As the plate dips and departs from the vertical position, the peaks become asymmetrical.

As the dip increases, the aspect ratio (Min/Max) decreases and this aspect ratio can be used as an empirical guide to dip angles from near 90º to about 30º. The method is not sensitive enough where dips are less than about 30º.

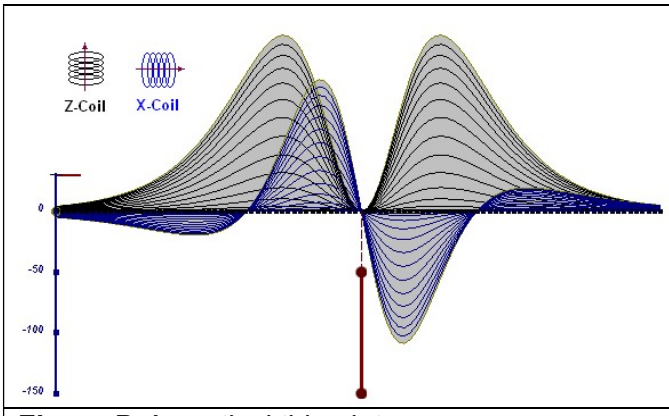

Figure D-1: vertical thin plate

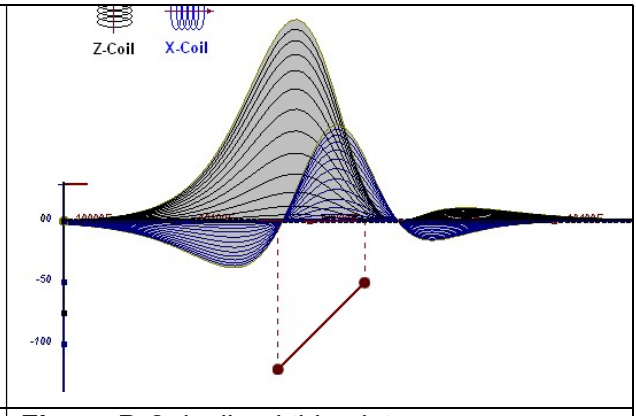

Figure D-2: inclined thin plate

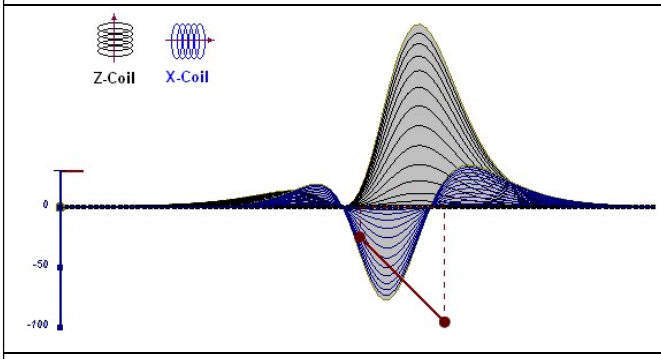

Figure D-3: inclined thin plate

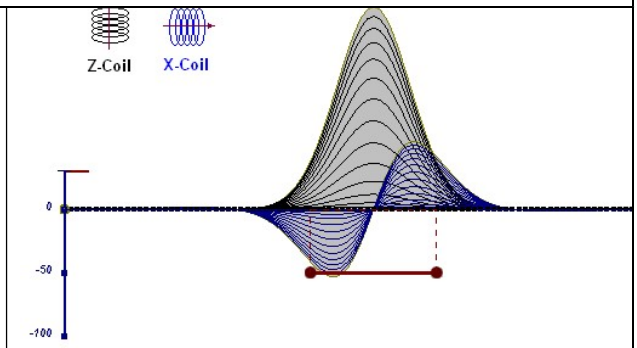

Figure D-4: horizontal thin plate

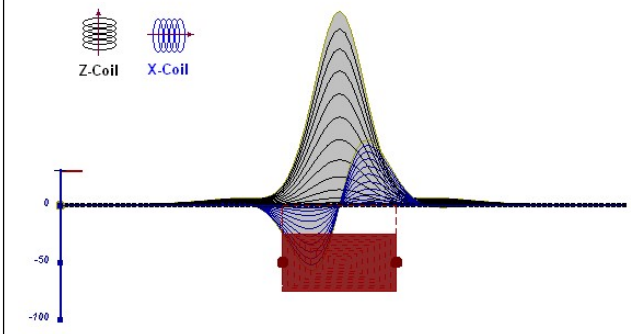

Figure D-5: horizontal thick plate (linear scale of the response)

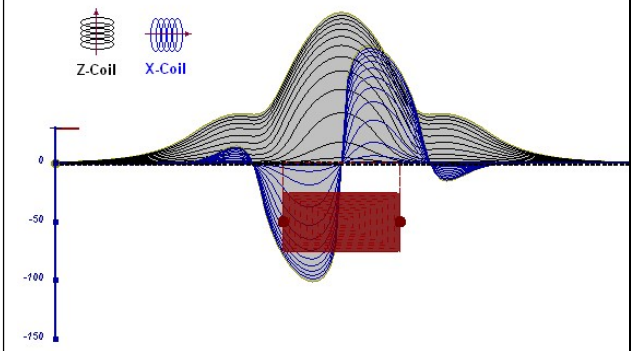

Figure D-6: horizontal thick plate (log scale of the response)

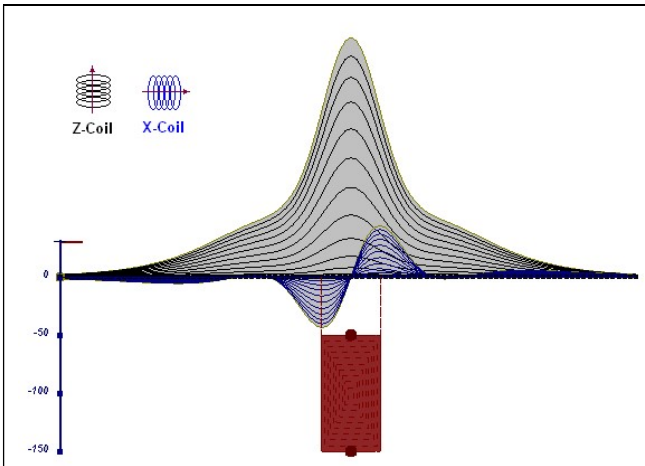

Figure D-7: vertical thick plate (linear scale of the response). 50 m depth

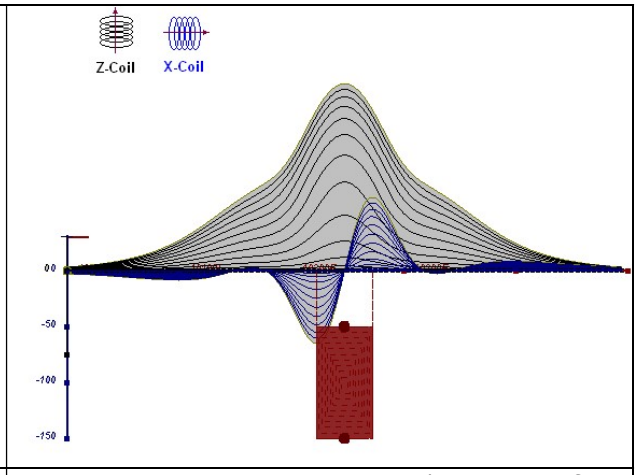

Figure D-8: vertical thick plate (log scale of the response). 50 m depth

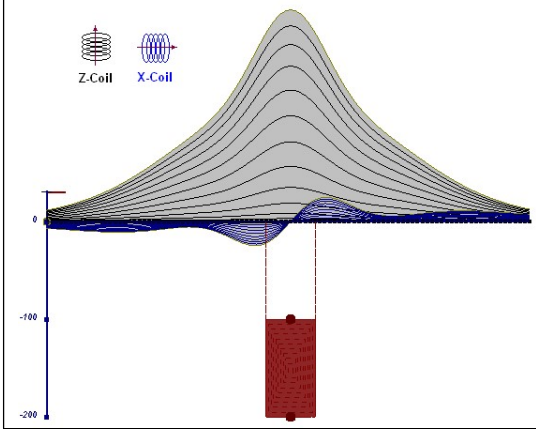

Figure D-9: vertical thick plate (linear scale of the response). 100 m depth

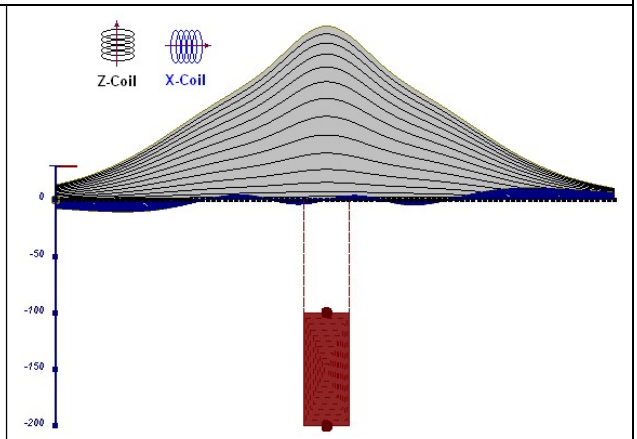

Figure D-10: vertical thick plate (linear scale of the response). Depth/hor.thickness=2.5

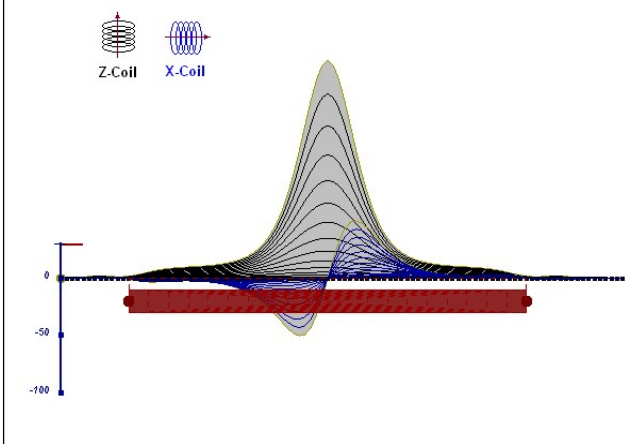

Figure D-10: horizontal thick plate (linear scale of the response)

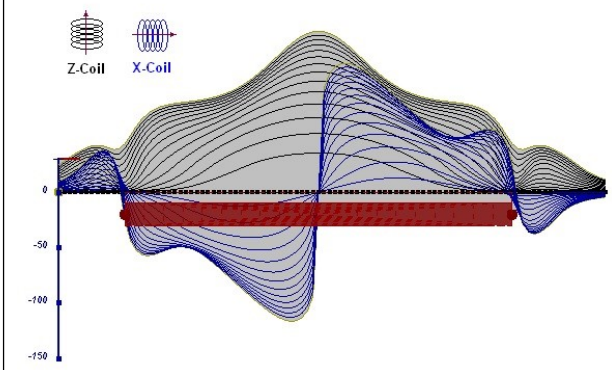

Figure D-11: horizontal thick plate (log scale of the response)

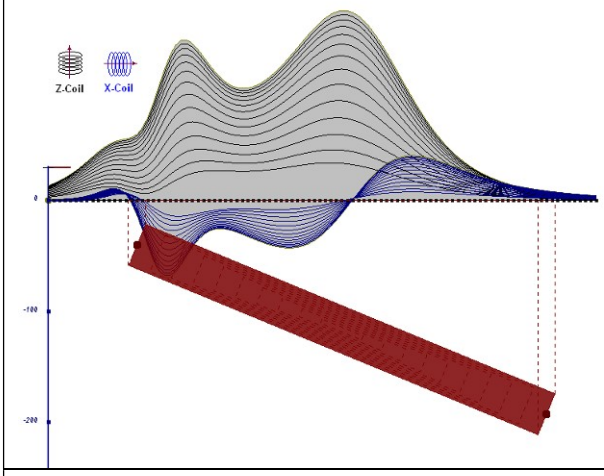

Figure D-12: inclined long thick plate

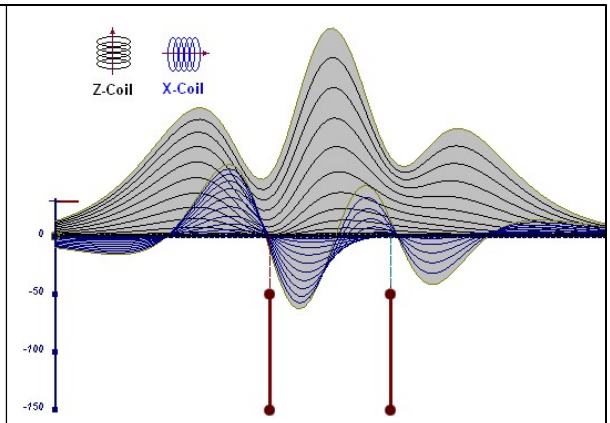

Figure D-13: two vertical thin plates

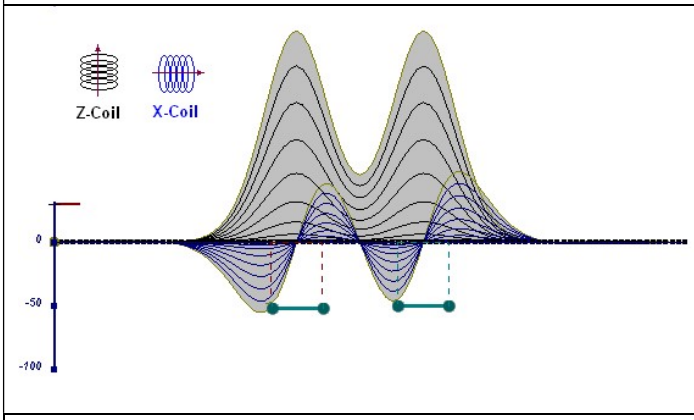

Figure D-14: two horizontal thin plates

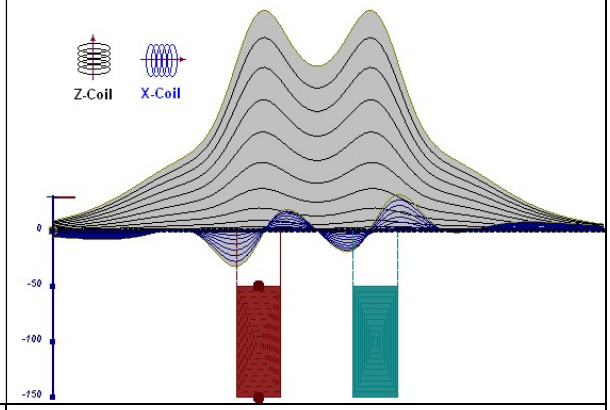

Figure D-15: two vertical thick plates

The same type of target but with different thickness, for example, creates different form of the response:

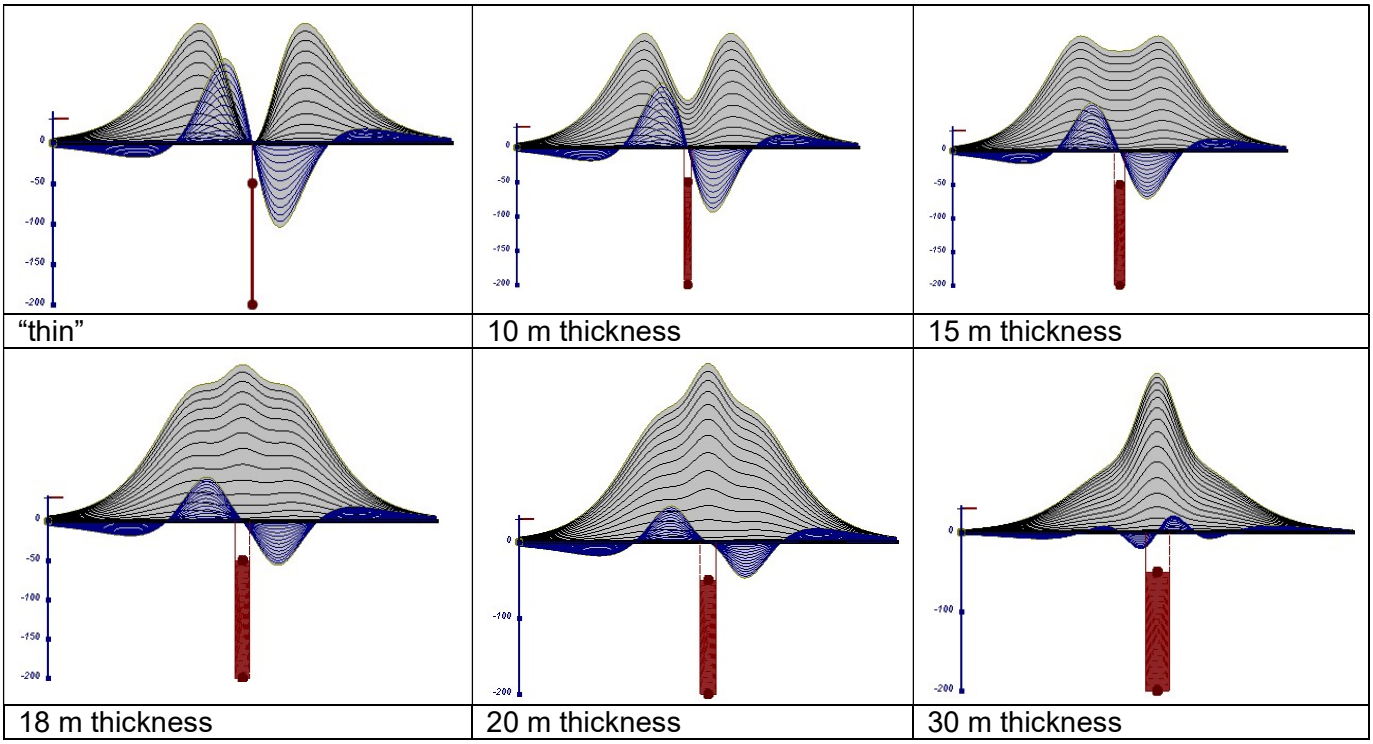

“thin”	10 m thickness	15 m thickness
18 m thickness	20 m thickness	30 m thickness

Figure D-16: Conductive vertical plate, depth 50 m, strike length 200 m, depth extend 150 m.

Alexander Prikhodko, PhD, P.Geo
UTS Ltd.

September 2010

APPENDIX E

EM TIME CONSTANT (TAU) ANALYSIS

Estimation of time constant parameter[1] in transient electromagnetic method is one of the steps toward the extraction of the information about conductances beneath the surface from TEM measurements.

The most reliable method to discriminate or rank conductors from overburden, background or one and other is by calculating the EM field decay time constant (TAU parameter), which directly depends on conductance despite their depth and accordingly amplitude of the response.

Theory

As established in electromagnetic theory, the magnitude of the electro-motive force (emf) induced is proportional to the time rate of change of primary magnetic field at the conductor. This emf causes eddy currents to flow in the conductor with a characteristic transient decay, whose Time Constant (Tau) is a function of the conductance of the survey target or conductivity and geometry (including dimensions) of the target. The decaying currents generate a proportional secondary magnetic field, the time rate of change of which is measured by the receiver coil as induced voltage during the Off time.

The receiver coil output voltage ($\mathbf{e_0}$) is proportional to the time rate of change of the secondary magnetic field and has the form,

$$e_0 \alpha (1 / \tau) e^{-(t/\tau)}$$

Where,
τ = L/R is the characteristic time constant of the target (TAU)
R = resistance
L = inductance

From the expression, conductive targets that have small value of resistance and hence large value of τ yield signals with small initial amplitude that decays relatively slowly with progress of time. Conversely, signals from poorly conducting targets that have large resistance value and smallτ, have high initial amplitude but decay rapidly with time[1] (Figure E-1).

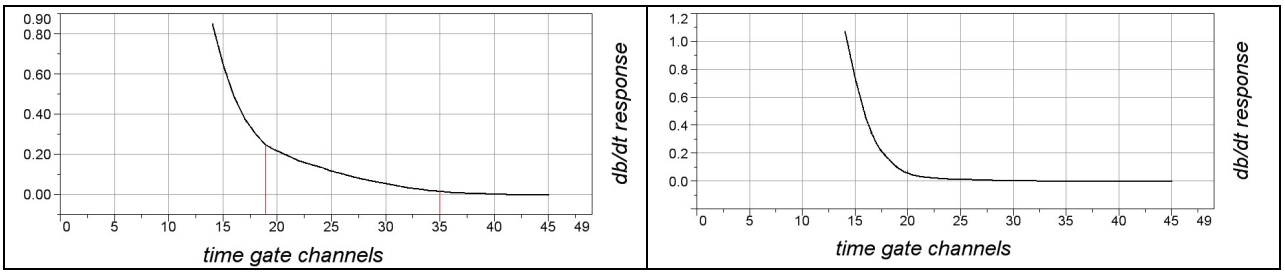

Figure E-1: Left – presence of good conductor, right – poor conductor.

[1] McNeill, JD, 1980, "Applications of Transient Electromagnetic Techniques", Technical Note TN-7 page 5, Geonics Limited, Mississauga, Ontario.

EM Time Constant (Tau) Calculation

The EM Time-Constant (TAU) is a general measure of the speed of decay of the electromagnetic response and indicates the presence of eddy currents in conductive sources as well as reflecting the "conductance quality" of a source. Although TAU can be calculated using either the measured dB/dt decay or the calculated B-field decay, dB/dt is commonly preferred due to better stability (S/N) relating to signal noise. Generally, TAU calculated on base of early time response reflects both near surface overburden and poor conductors whereas, in the late ranges of time, deep and more conductive sources, respectively. For example early time TAU distribution in an area that indicates conductive overburden is shown in Figure 2.

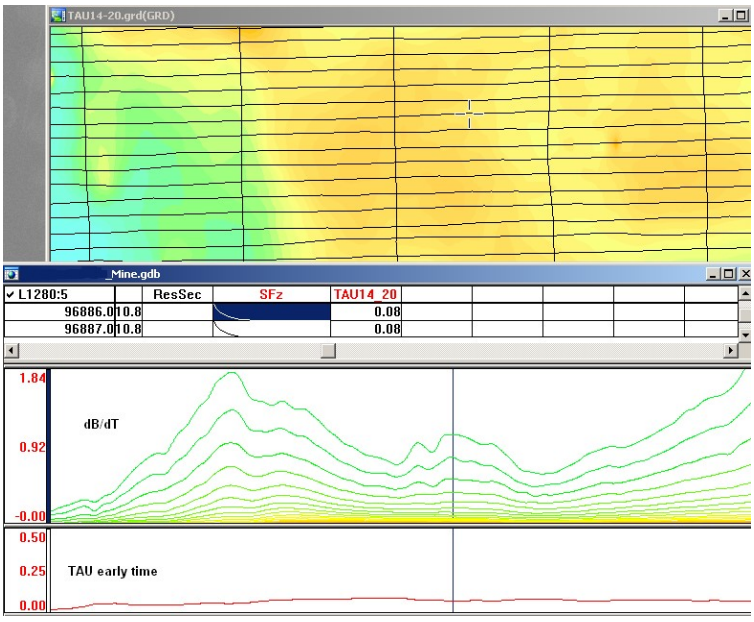

Figure E-2: Map of early time TAU. Area with overburden conductive layer and local sources.

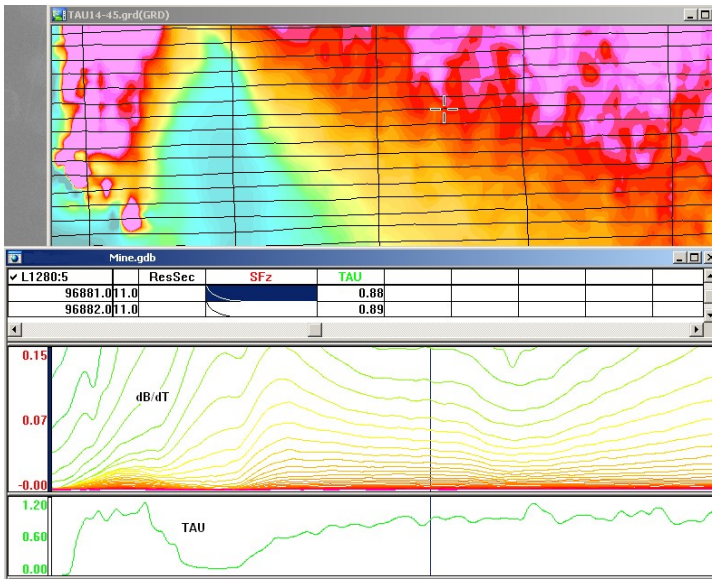

Figure E-3: Map of full time range TAU with EM anomaly due to deep highly conductive target.

There are many advantages of TAU maps:

- TAU depends only on one parameter (conductance) in contrast to response magnitude;
- TAU is integral parameter, which covers time range and all conductive zones and targets are displayed independently of their depth and conductivity on a single map.
- Very good differential resolution in complex conductive places with many sources with different conductivity.
- Signs of the presence of good conductive targets are amplified and emphasized independently of their depth and level of response accordingly.

In the example shown in Figure 4 and 5, three local targets are defined, each of them with a different depth of burial, as indicated on the resistivity depth image (RDI). All are very good conductors but the deeper target (number 2) has a relatively weak dB/dt signal yet also features the strongest total TAU (Figure 4). This example highlights the benefit of TAU analysis in terms of an additional target discrimination tool.

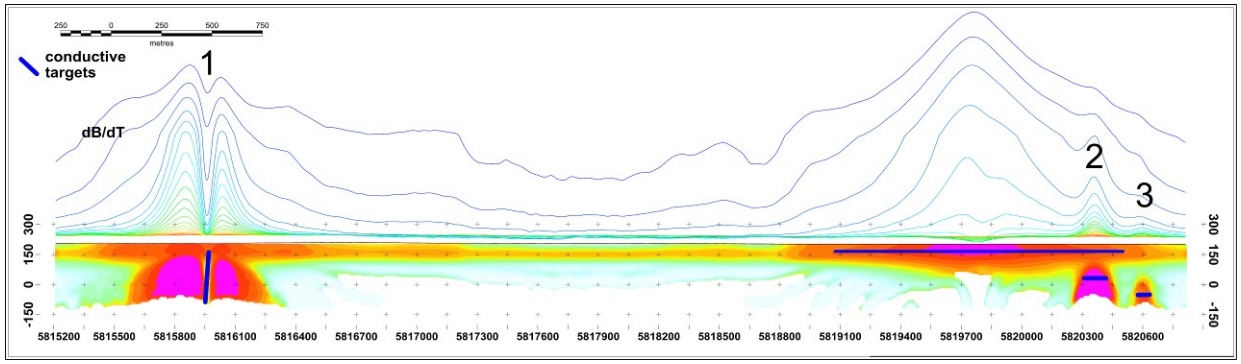

Figure E-4: dB/dt profile and RDI with different depths of targets.

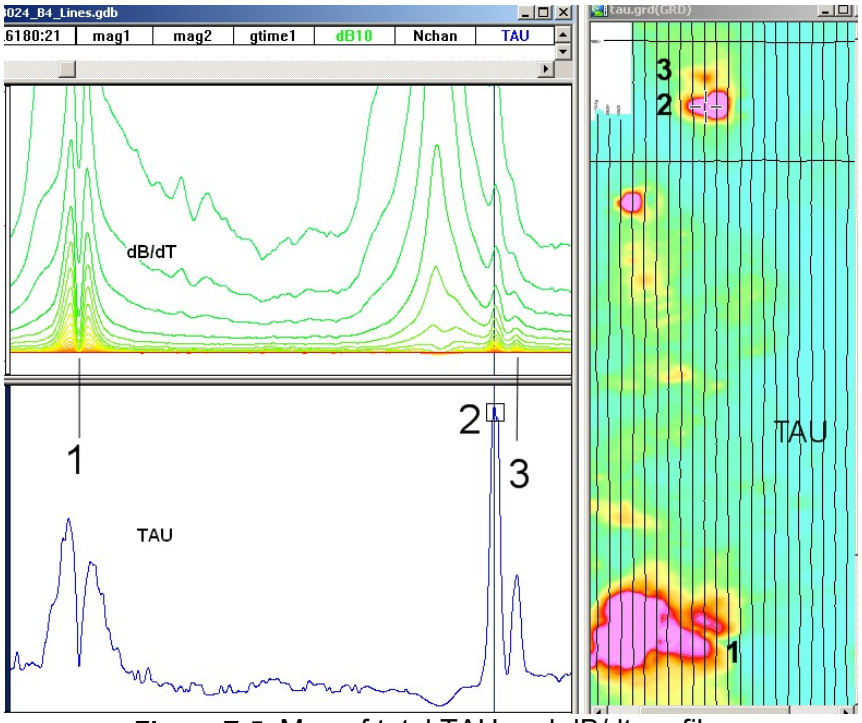

Figure E-5: Map of total TAU and dB/dt profile.

The EM Time Constants for dB/dt and B-field were calculated using the "sliding Tau" in-house program developed at UTS[2]. The principle of the calculation is based on using of time window (4 time channels) which is sliding along the curve decay and looking for latest time channels which have a response above the level of noise and decay. The EM decays are obtained from all available decay channels, starting at the latest channel. Time constants are taken from a least square fit of a straight-line (log/linear space) over the last 4 gates above a pre-set signal threshold level (Figure F6). Threshold settings are pointed in the "label" property of TAU database channels. The sliding Tau method determines that, as the amplitudes increase, the time-constant is taken at progressively later times in the EM decay. Conversely, as the amplitudes decrease, Tau is taken at progressively earlier times in the decay. If the maximum signal amplitude falls below the threshold, or becomes negative for any of the 4 time gates, then Tau is not calculated and is assigned a value of "dummy" by default.

[2] by A.Prikhodko

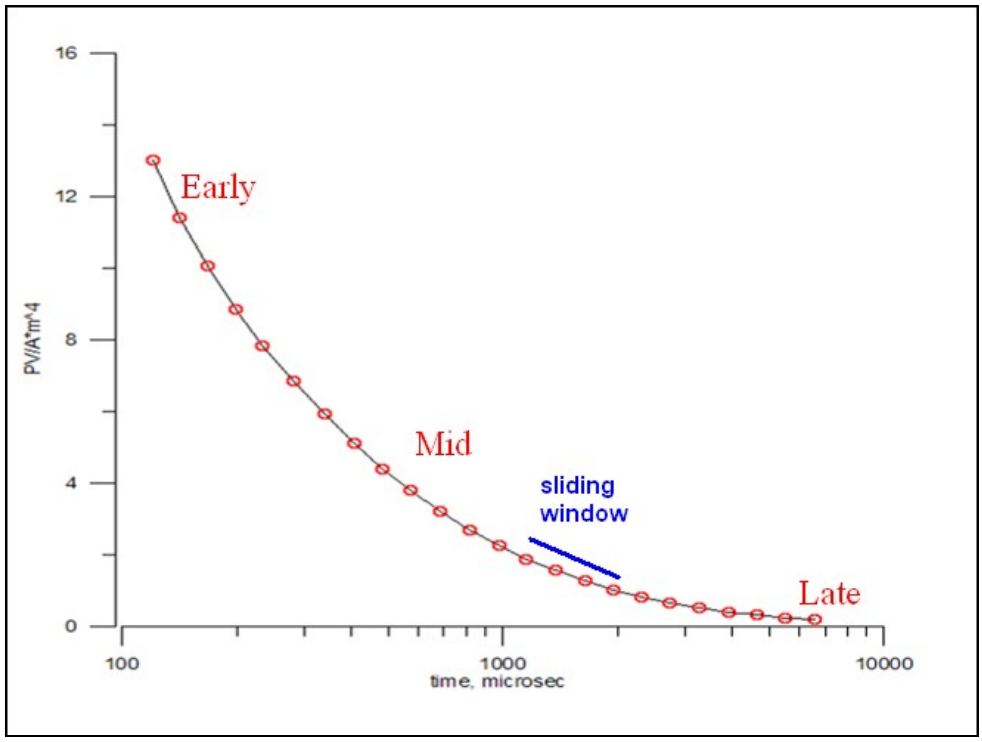

Figure E-6: Typical dB/dt decays of VTEM^{TM} data

Alexander Prikhodko, PhD, P.Geo
UTS Ltd.

September 2010

APPENDIX F

TEM RESISTIVITY DEPTH IMAGING (RDI)

Resistivity depth imaging (RDI) is technique used to rapidly convert EM profile decay data into an equiVenture Minerals Ltd.nt resistivity versus depth cross-section, by deconvolving the measured TEM data.
The used RDI algorithm of Resistivity-Depth transformation is based on scheme of the apparent resistivity transform of Maxwell A.Meju (1998)[1] and TEM response from conductive half-space. The program is developed by Alexander Prikhodko and depth calibrated based on forward plate modeling for VTEM™ system configuration (Fig. 1-10).

RDIs provide reasonable indications of conductor relative depth and vertical extent, as well as accurate 1D layered-earth apparent conductivity/resistivity structure across VTEM™ flight lines. Approximate depth of investigation of a TEM system, image of secondary field distribution in half space, effective resistivity, initial geometry and position of conductive targets is the information obtained on base of the RDIs.

Maxwell forward modeling with RDI sections from the synthetic responses (VTEM™ system)

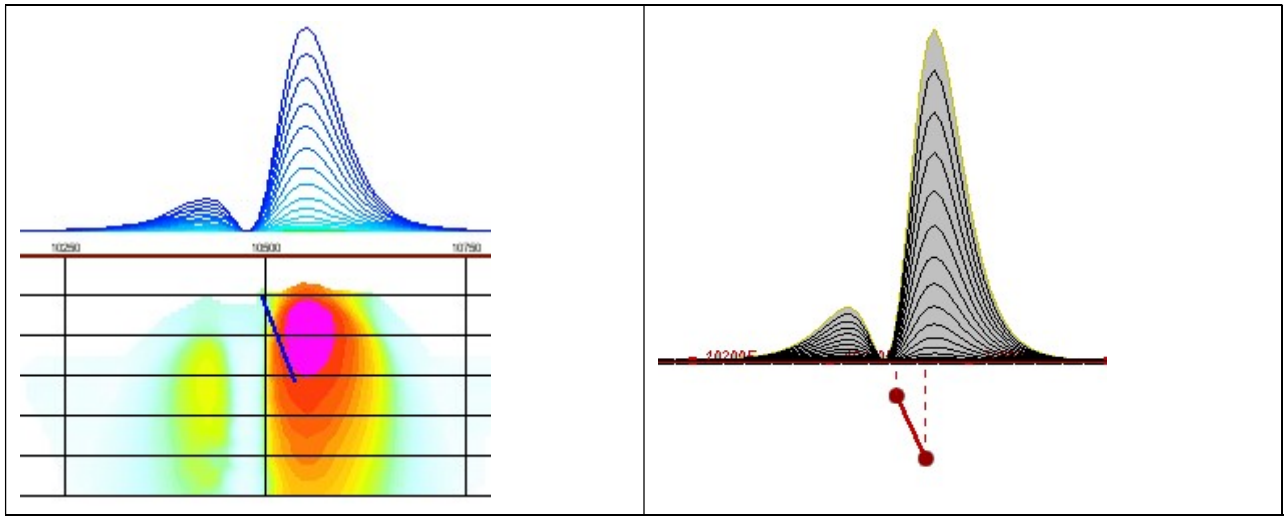

Figure F-1: Maxwell plate model and RDI from the calculated response for conductive “thin” plate (depth 50 m, dip 65 degree, depth extend 100 m).

[1] Maxwell A.Meju, 1998, Short Note: A simple method of transient electromagnetic data analysis, Geophysics, **63**, 405–410.

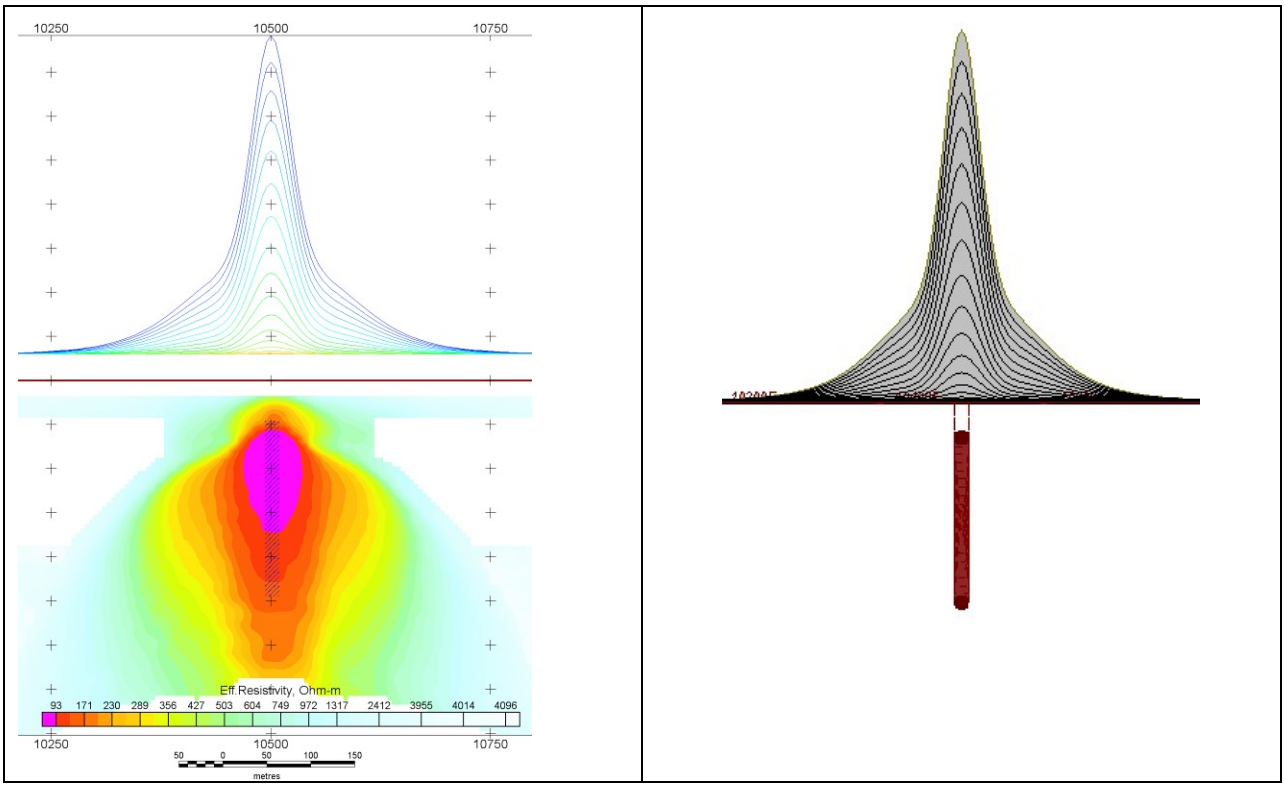

Figure F-2: Maxwell plate model and RDI from the calculated response for “thick” plate 18 m thickness, depth 50 m, depth extend 200 m).

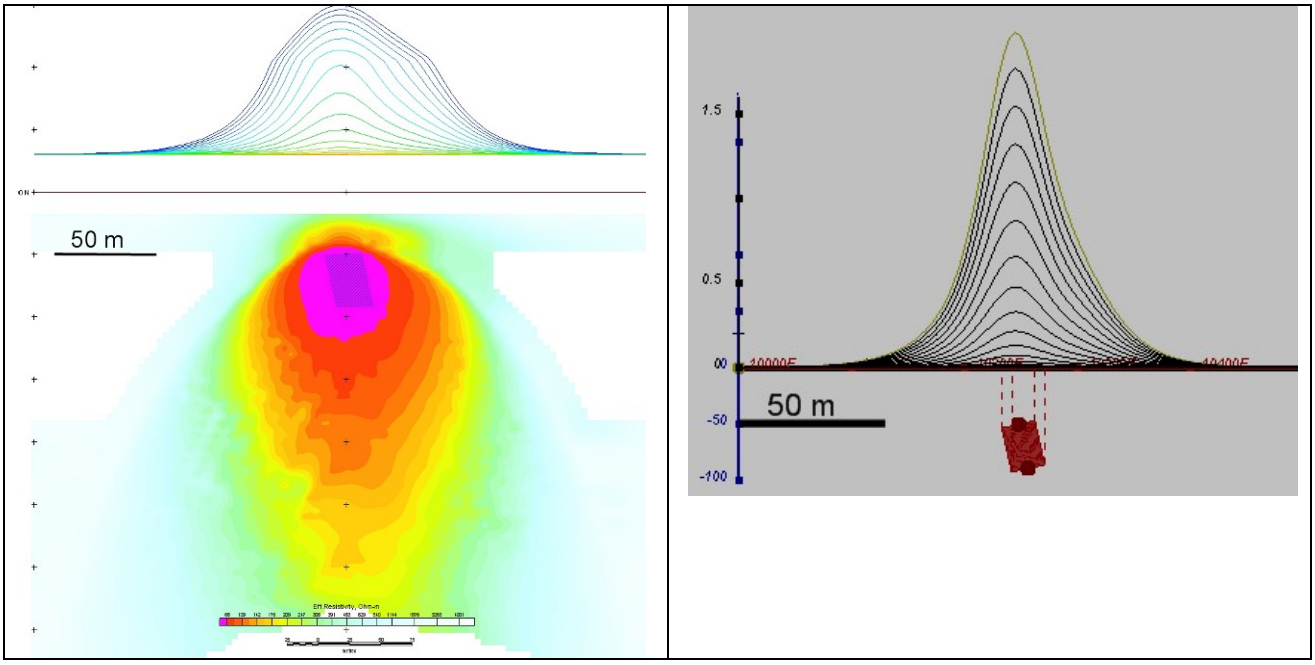

Figure F-3: Maxwell plate model and RDI from the calculated response for bulk (“thick”) 100 m

length, 40 m depth extend, 30 m thickness

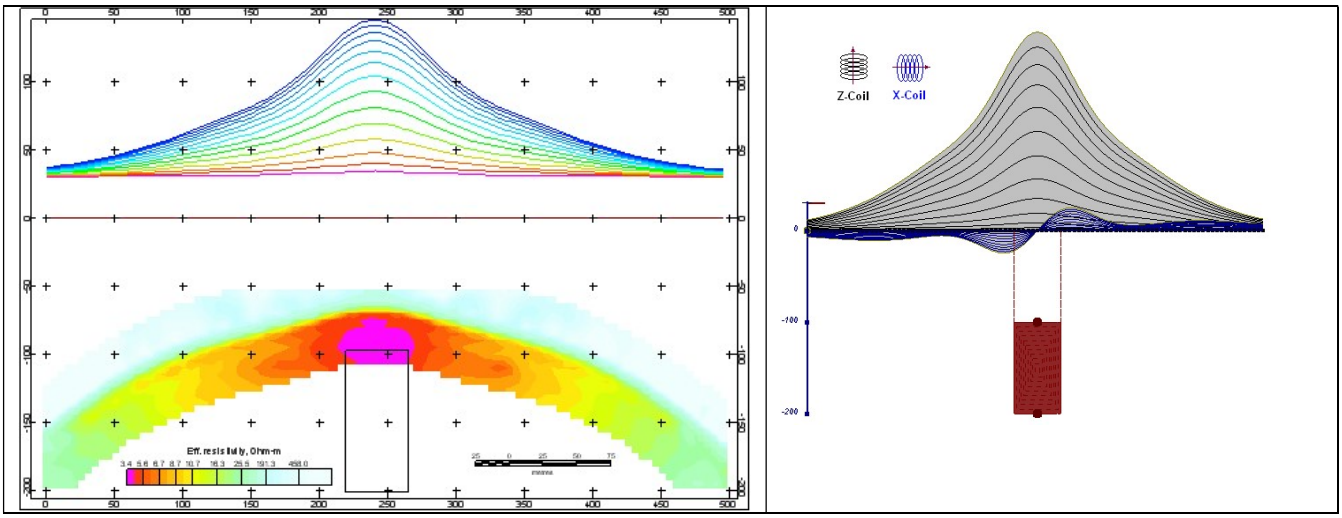

Figure F-4: Maxwell plate model and RDI from the calculated response for “thick” vertical target (depth 100 m, depth extend 100 m). 19-44 chan.

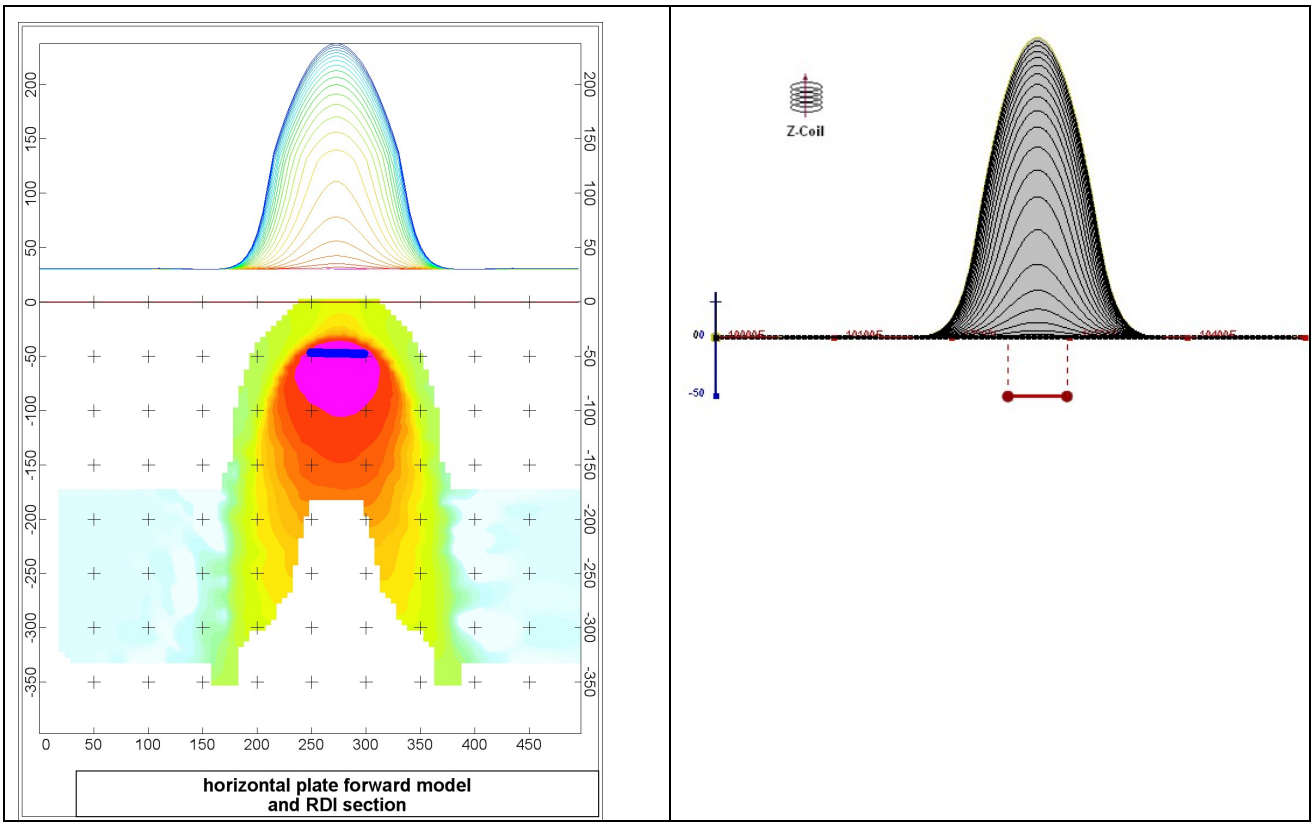

Figure F-5: Maxwell plate model and RDI from the calculated response for horizontal thin plate (depth 50 m, dim 50x100 m). 15-44 chan.

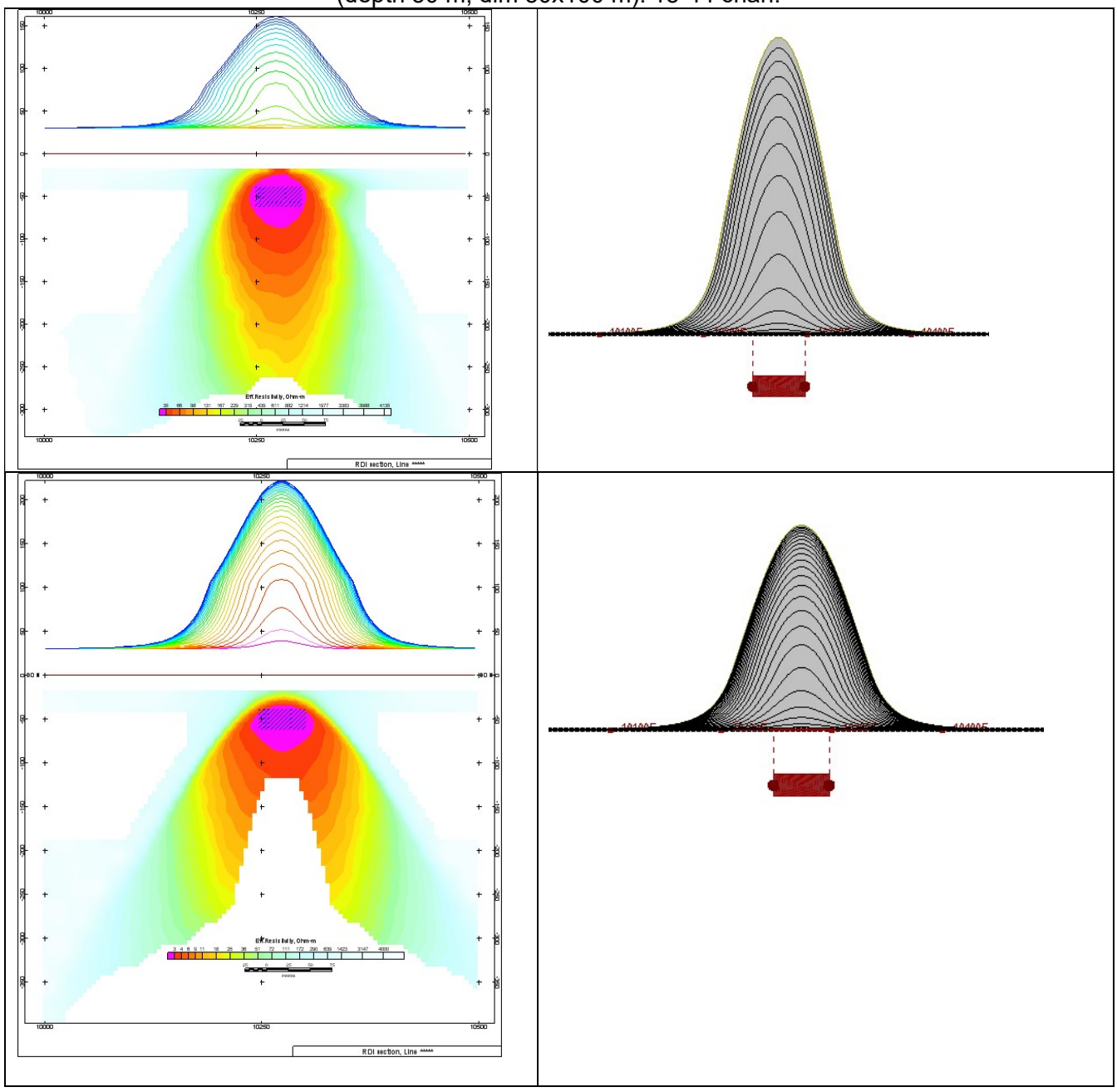

Figure F-6: Maxwell plate model and RDI from the calculated response for horizontal thick (20m) plate – less conductive (on the top), more conductive (below)

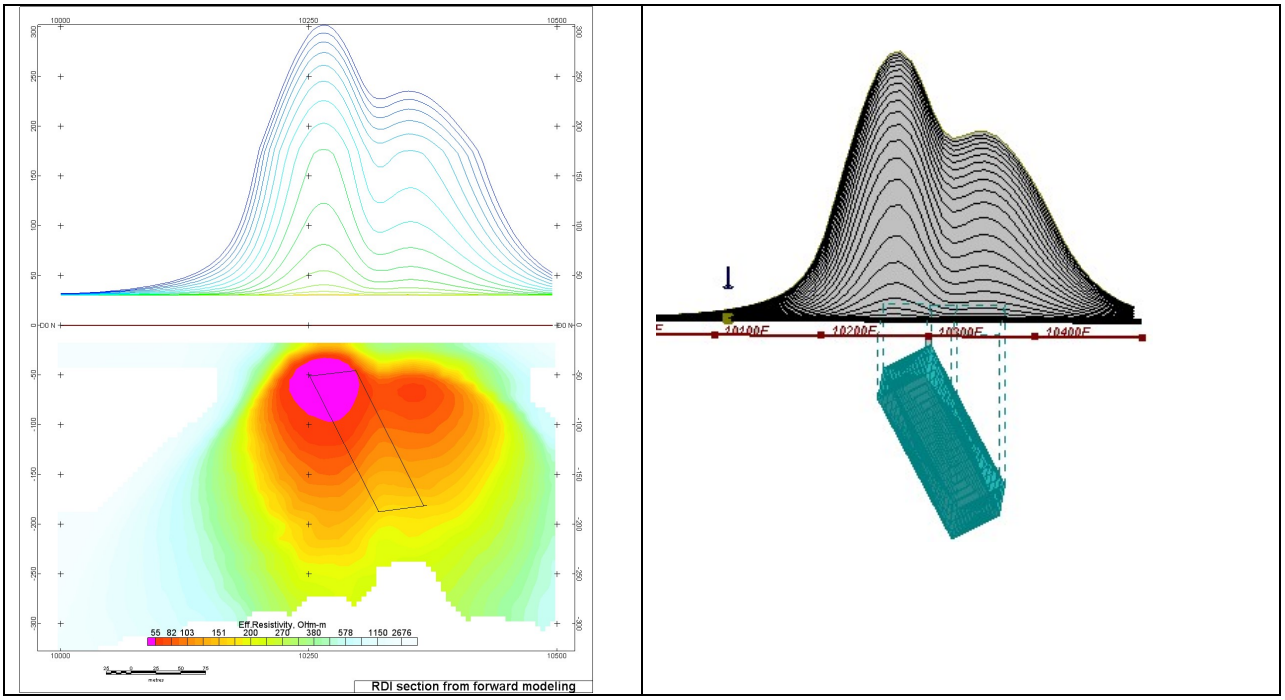

Figure F-7: Maxwell plate model and RDI from the calculated response for inclined thick (50m) plate. Depth extends 150 m, depth to the target 50 m.

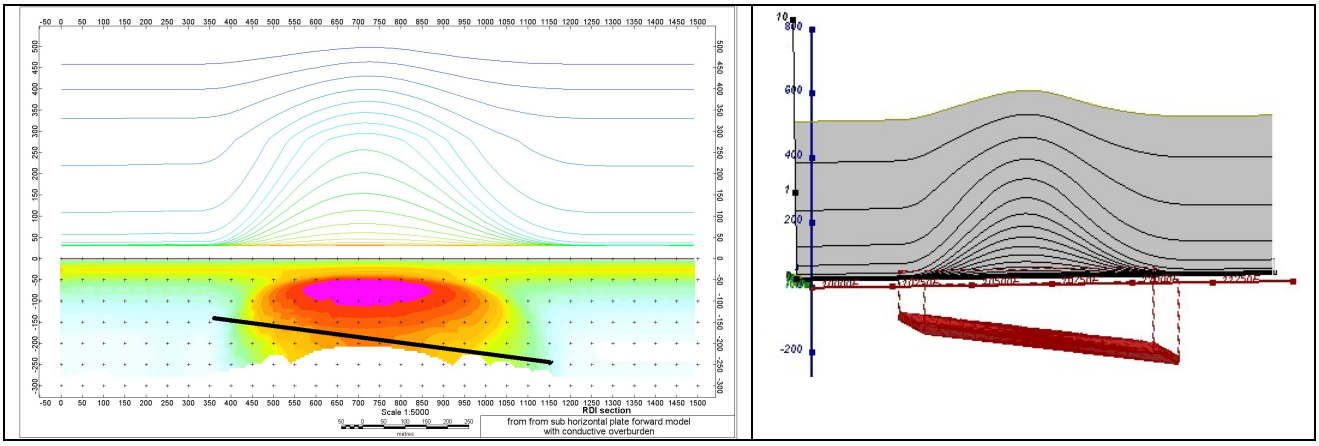

Figure F-8: Maxwell plate model and RDI from the calculated response for the long, wide and deep subhorizontal plate (depth 140 m, dim 25x500x800 m) with conductive overburden.

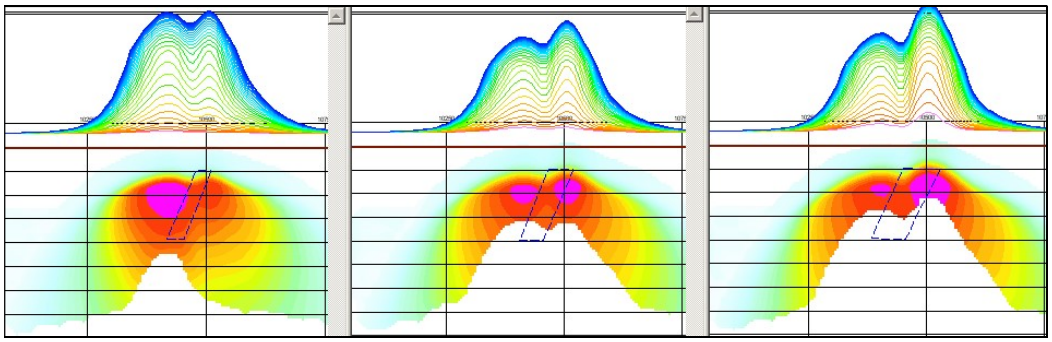

Figure F-9: Maxwell plate models and RDIs from the calculated response for “thick” dipping plates (35, 50, 75 m thickness), depth 50 m, conductivity 2.5 S/m.

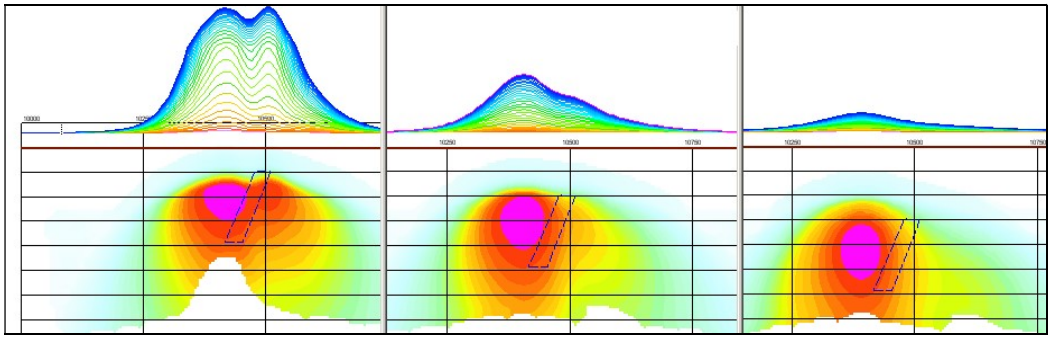

Figure F-10: Maxwell plate models and RDIs from the calculated response for “thick” (35 m thickness) dipping plate on different depth (50, 100, 150 m), conductivity 2.5 S/m.

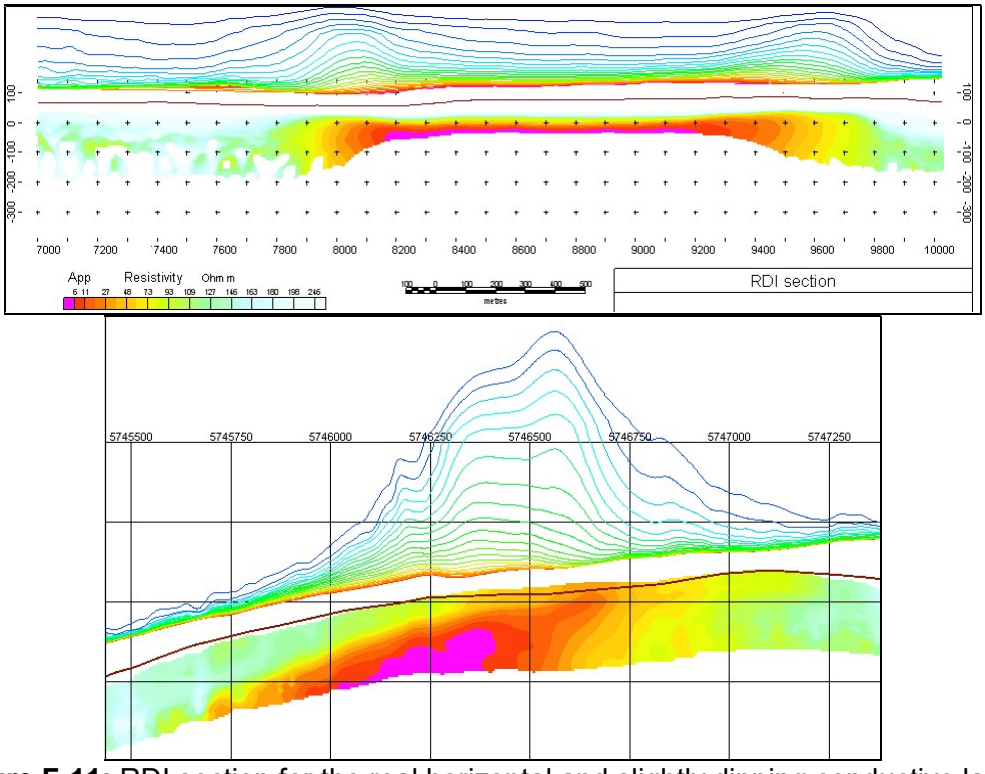

Figure F-11: RDI section for the real horizontal and slightly dipping conductive layers

FORMS OF RDI PRESENTATION

Presentation of series of lines

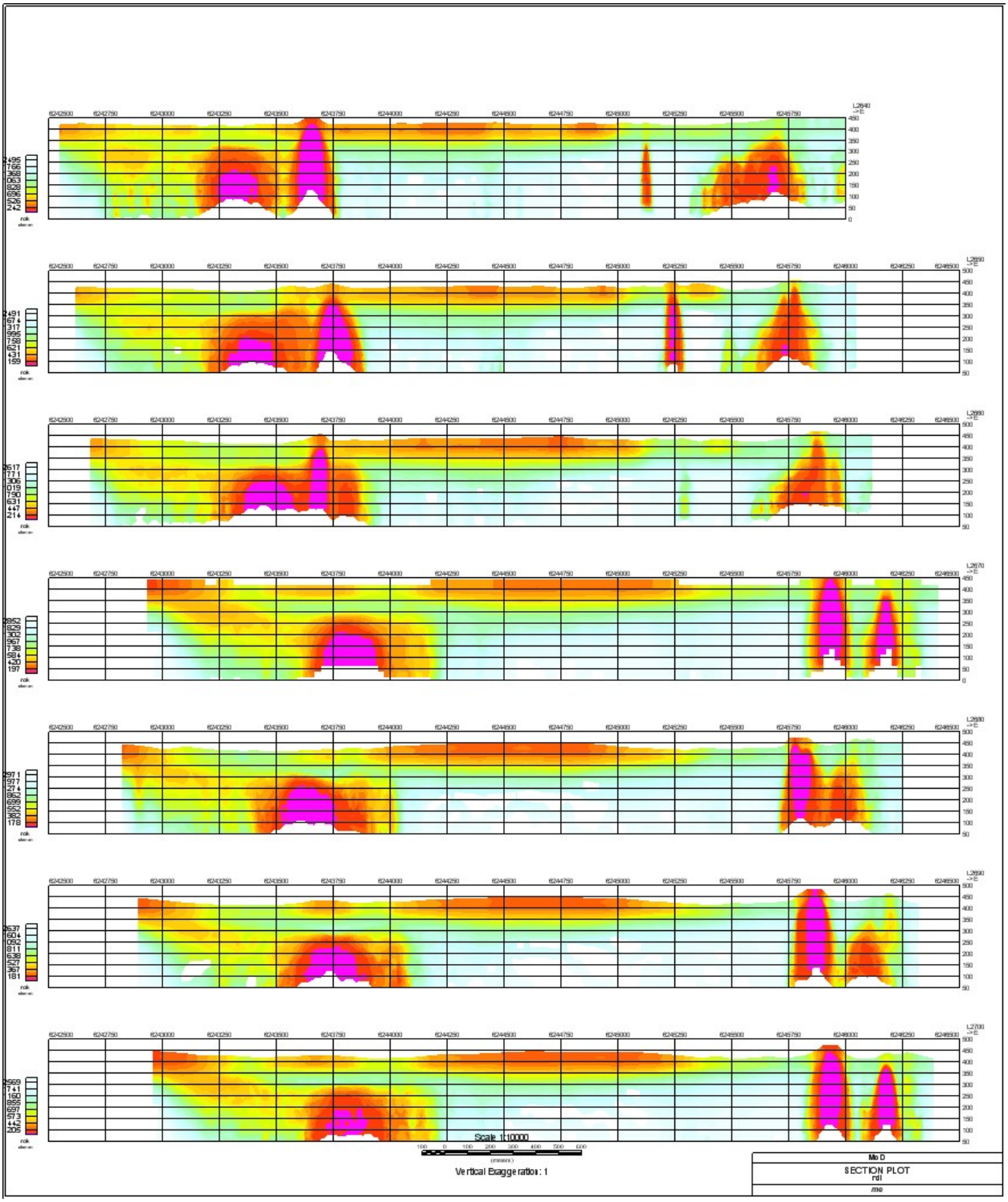

3d presentation of RDIs

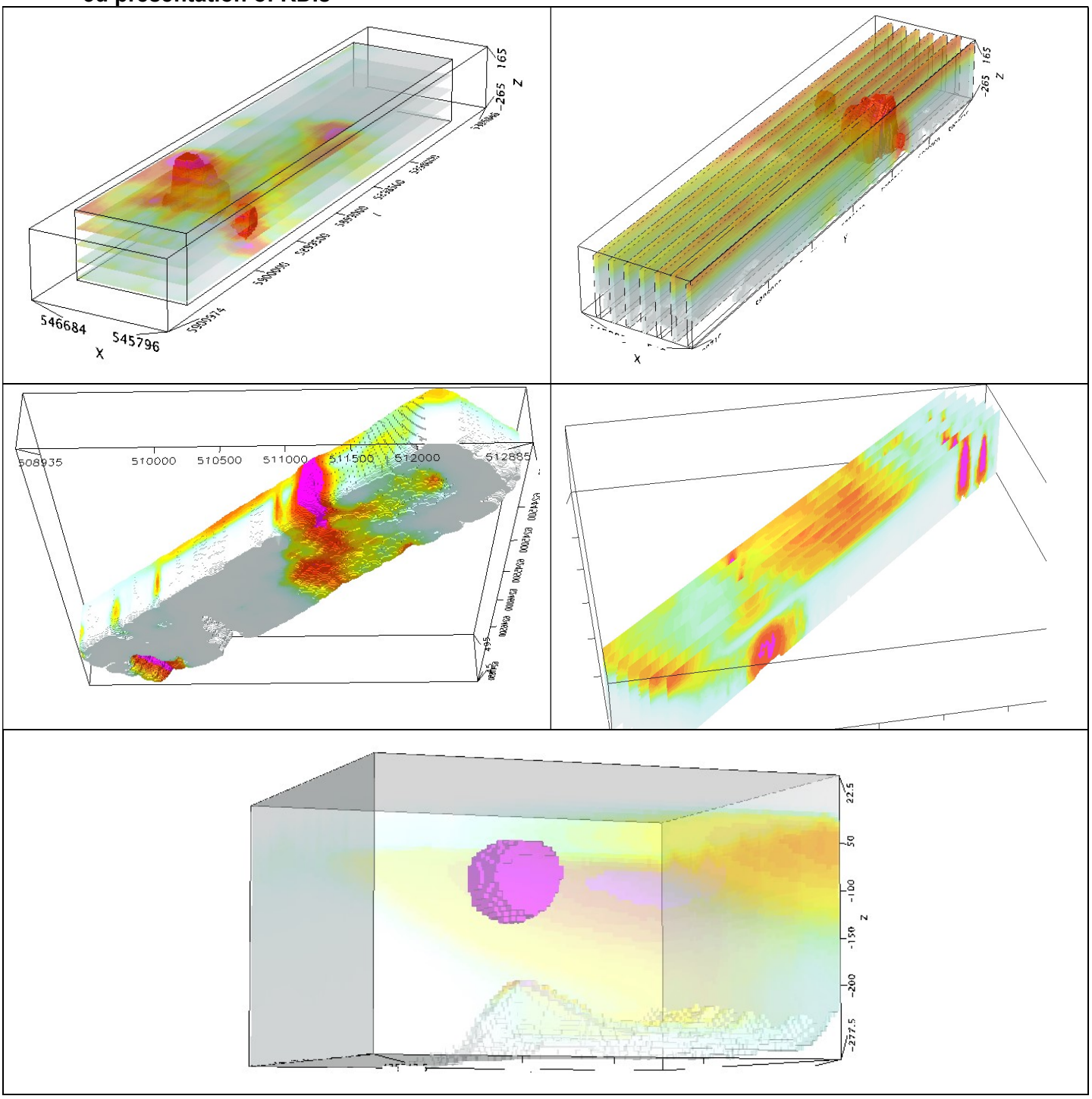

Apparent Resistivity Depth Slices plans:

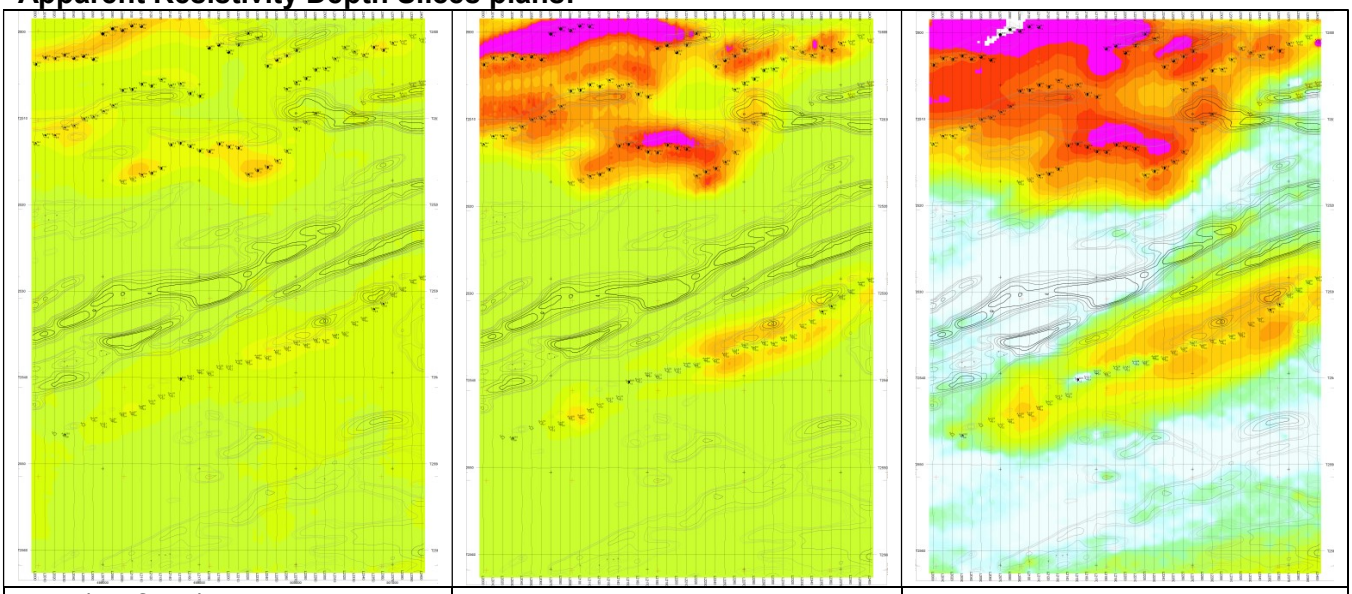

0 m (surface)	-100 m	-200 m

3d views of apparent resistivity depth slices:

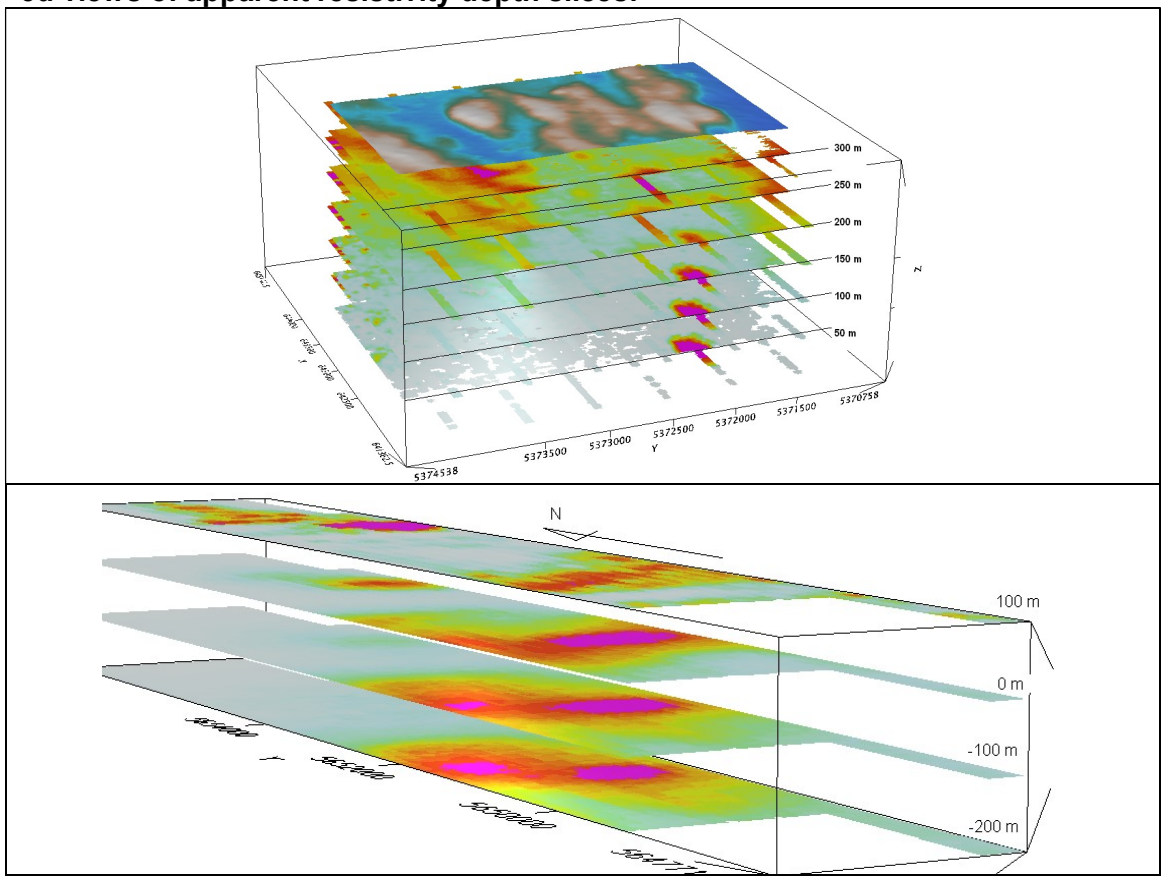

Real base metal targets in comparison with RDIs:

RDI section of the line over Caber deposit (“thin” subvertical plate target and conductive overburden).

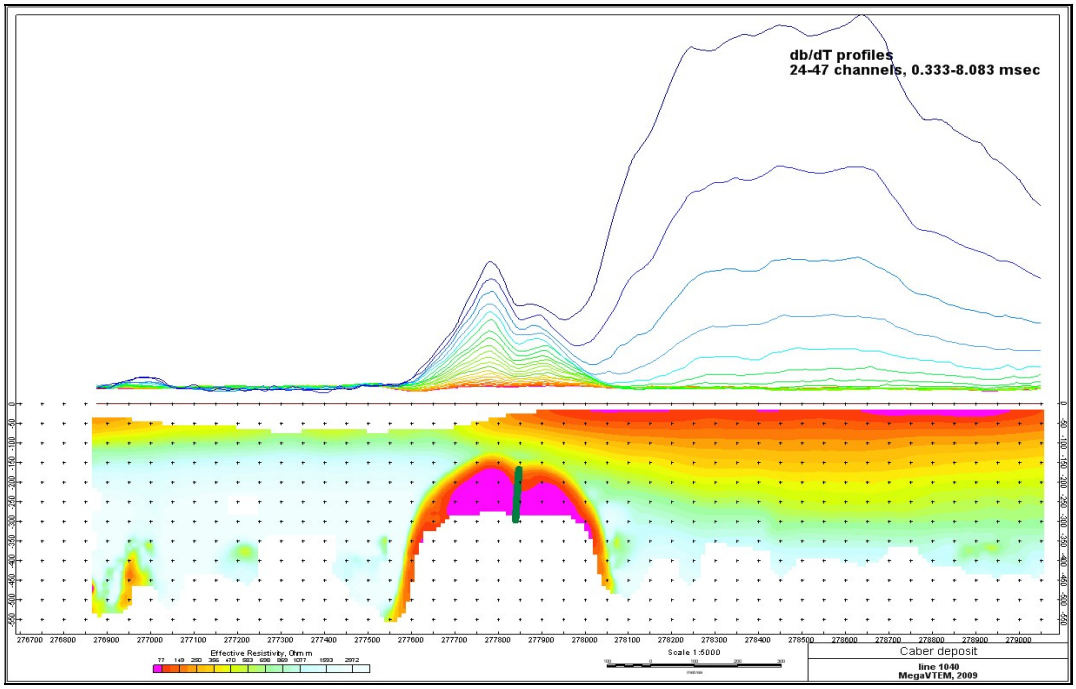

3d RDI voxels with base metals ore bodies (Middle East):

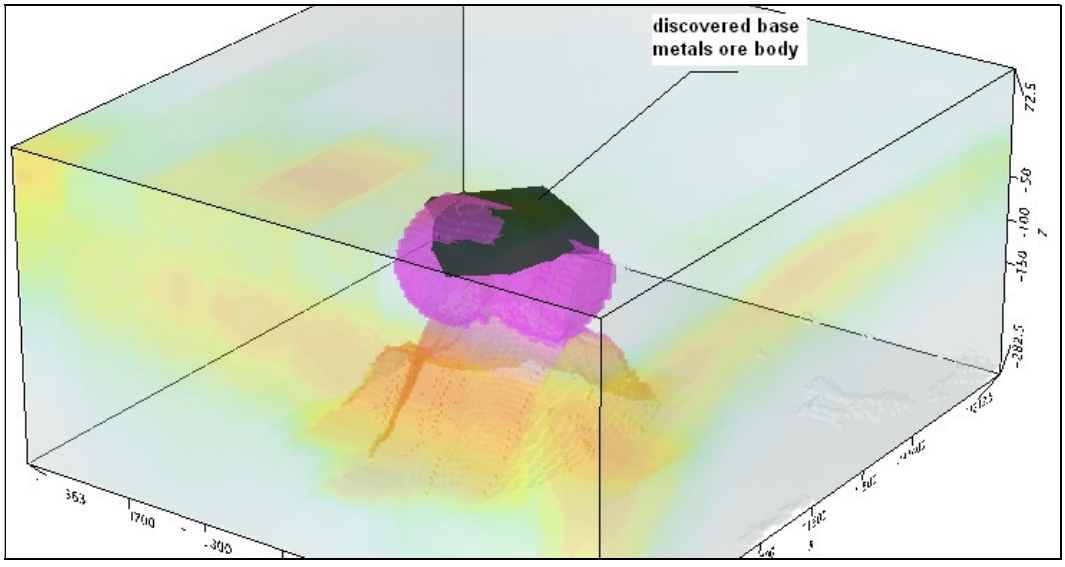

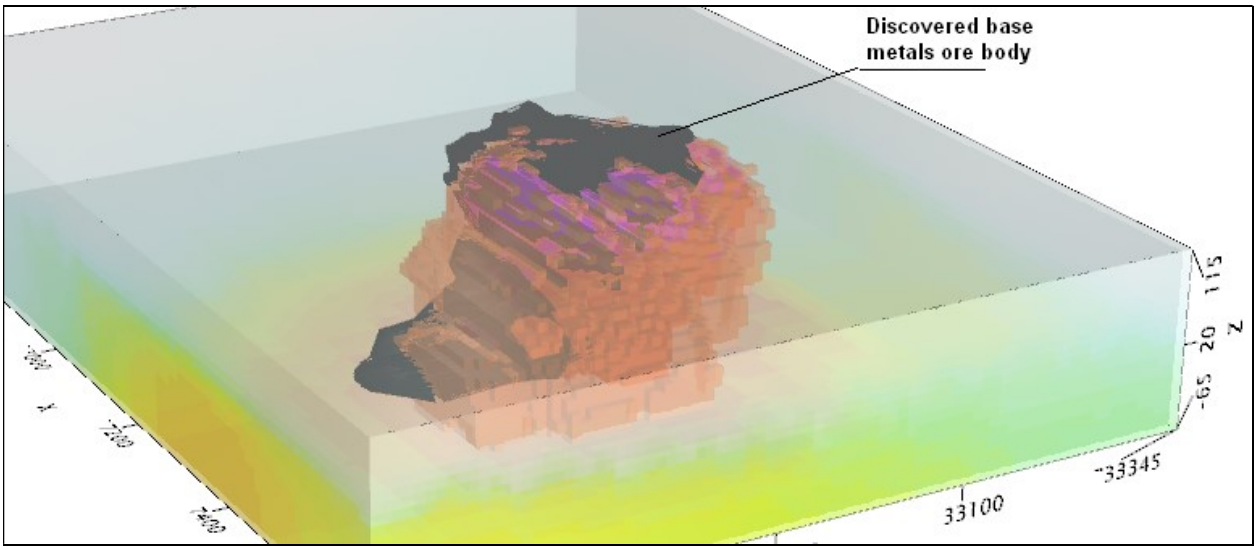

Alexander Prikhodko, PhD, P.Geo
UTS Ltd.
April 2011

APPENDIX H

Resistivity Depth Images (RDI)

Please see attached DVD for each block RDI.